AD-A189 560

①

THRESHOLD FATIGUE CRACK GROWTH

IN Ti-6A1-2Sn-4Zr-6Mo

THESIS

Dale A. Nagy
Captain, USAF

AFIT/GAE/AA/87D-13

DEPARTMENT OF THE AIR FORCE

AIR UNIVERSITY

AIR FORCE INSTITUTE OF TECHNOLOGY

Wright-Patterson Air Force Base, Ohio

88 3 01 177

THRESHOLD FATIGUE CRACK GROWTH

IN Ti-6Al-2Sn-4Zr-6Mo

THESIS

Dale A. Nagy
Captain, USAF

AFIT/GAE/AA/87D-13

DTIC
ELECTE
S
MAR 0 3 1988
D
H

AFIT/GAE/AA/87D-13

THRESHOLD FATIGUE CRACK GROWTH IN Ti-6Al-2Sn-4ZR-6Mo

THESIS

Presented to the Faculty of the School of Engineering

of the Air Force Institute of Technology

Air University

In Partial Fulfillment of the

Requirements of the Degree of

Master of Science in Aeronautical Engineering

Dale A. Nagy, B.S.

Captain, USAF

December 1987

Preface

The purpose of this study was to investigate the effects of loading history, closure loads, and varying stress ratios on the crack growth rate of Ti-6Al-2Sn-4Zr-6Mo near the threshold growth level. This is necessary to predict the material life of structures subject to fatigue crack growth.

Tests were conducted on this material to investigate loading history effects on the near-threshold growth rate. Results indicate that different loading histories and stress ratios produce similar crack growth rate curves and threshold stress intensities when adjusted for closure, using ΔK_{eff}.

I would like to thank my advisor, Dr. S. Mall for his patience and guidance. I would also like to thank Jay Jira and Dr. Ted Nicholas of the Materials Lab for the support and assistance without which the experimentation and data analysis would never have been finished. Finally, I would like to thank my wife Jan for the cookies and kisses that kept me going through the night .

<div align="right">Dale A. Nagy</div>

11

Table of Contents

List of Figures

List of Tables

vi

Abstract

The purpose of this study was to examine the effects of different loading histories, closure loads, and stress ratios on the near-threshold crack growth rate of a Ti-Al alloy. Two different test types were conducted on four separate specimens to determine the threshold stress intensity of the material. The first test type maintained a constant maximum stress intensity factor, K_{max}, on a specimen with a growing crack. As the crack grew, the minimum stress intensity factor was increased until the crack growth rate reached the threshold level ($1*10^{-10}$ m/cycle). The second test type also maintained a constant K_{max}. For this test a block of cycles was applied to the specimen and if the crack growth rate for the block of cycles was below the threshold level ($5*10^{-11}$) then K_{min} was decreased by a small amount and another block of cycles was applied. This processed was continued until the crack growth rate reached the threshold level. Once the threshold stress intensity was determined the cracks were grown under constant maximum load and stress ratio (R) to measure the threshold crack growth rate. Both test types were conducted over a wide range of stress ratios to investigate the effects of varying closure loads.

An MTS machine was used to apply the fatigue cycles to the specimen and a laser interferometer displacement gage (IDG) was used to measure compliance crack growth and the closure loads for the specimen.

The results of these tests were compared to the results of a previous study using the ASTM standard threshold measurement tests (constant R and decreasing ΔK) and another commonly used threshold test (constant R and increasing ΔK). Analysis of the data indicated that threshold stress intensity factors (ΔK_{th}) were _dependent_ on stress ratio. Threshold stress intensity factors adjusted for closure, ΔK_{effth}, were _not dependent_ on stress ratio.

The crack growth rate curves for all tests coincided in the near-threshold region ($1*10^{-9}$ to $1*10^{-10}$ m/cycle) when plotted versus ΔK_{eff}. Finally, the laser IDG had difficulty measuring closure loads while transitioning from a condition of large closure loads (usually $R \leq 0.1$) to a condition of no closure ($R \geq 0.5$).

THRESHOLD FATIGUE CRACK GROWTH IN Ti-6Al-2Sn-4Zr-6Mo

I. Introduction

Overview

The structural materials used in today's aircraft and
turbine engines are subject to high cycle fatigue crack
growth, particularly in the near-threshold region (10^{-10}
m/cycle). It is crucial to determine the near-threshold crack
growth behavior for these high cycle fatigue limited
components for accurate life predictions. In addition to
determining near-threshold crack growth, calculating the
threshold stress intensity below which a crack will not grow
(ΔK_{th}), is important in predicting component life.

Background

The Paris-Erdogan equation is currently used to predict
fatigue crack growth in a structure:

$$da/dN = A\ \Delta K^{n} \tag{1}$$

where da/dN is the crack growth rate, ΔK is the stress
intensity factor, and A and n are material constants. This
equation does not accurately model the near-threshold crack
growth region. To modify this equation there is a need to
determine a material constant, similar to A and n , for the
near-threshold regime. One possibility that has been
investigated is the threshold stress intensity factor, ΔK_{th}.

The ASTM recommended method (1:248) for determining ΔK_{th}
is a load shedding test (see Figure 1a). During the load

1

a. DECREASING ΔK THRESHOLD TEST

b. INCREASING ΔK THRESHOLD TEST
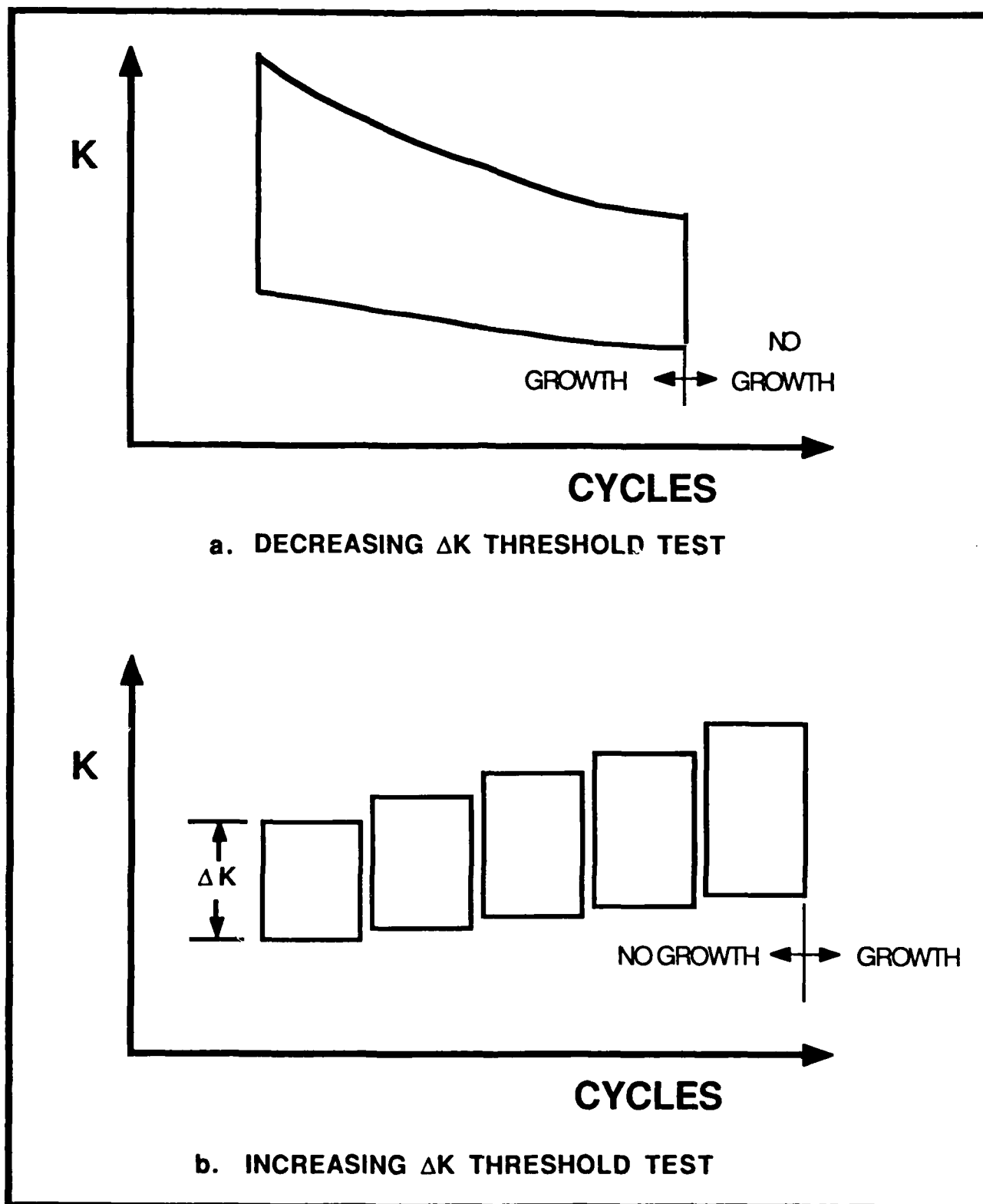
Figure 1. Constant Stress Ratio Tests

2

shedding test a specimen with a propagating crack is subject
to a decreasing stress intensity, ΔK, at a constant stress
ratio, R ($\sigma_{min}/\sigma_{max}$). This results in a decreasing crack
growth rate. The ΔK_{th} is, then, determined when the crack
growth rate reaches the threshold level of 10^{-10} m/cycle.
Tests attempting to measure a standard ΔK_{th} to be used for
material life predictions have found threshold stress
intensity values varying up to 40% (2:59-75) depending on
reduction rate of ΔK, test frequency, environment, and stress
ratio. These researchers, therefore, concluded that the
measured ΔK_{th} values are very dependent on loading history,
crack closure, and plastic zone size.

Later researchers (3:6) found that crack growth rates
obtained at different stress ratios tend to merge to a single
curve using a stress intensity adjusted for crack closure,
$\Delta K_{eff} = K_{max} - K_{cl}$. These researchers also found that
effective threshold stress intensity values, ΔK_{effth}, were
approximately equal for different stress ratios. This study
showed the possibility of using ΔK_{effth} as a material property
in the near-threshold crack growth region.

There is obviously a need to determine if similar
results are obtained under different loading histories, and
crack closure effects. In addition, there is a need to
determine if results obtained from threshold tests with
initially propagating cracks are applicable to materials with
initially non-propagating cracks.

3

Approach

To examine the effects of closure and loading history on
crack growth rate and ΔK_{th}, the present study was undertaken.
This study compares four different test types conducted on a
high strength titanium alloy, Ti 6Al-2Sn-4Zr-6Mo, with a
surface flaw. Each test type was run with different stress
ratios (R) to produce different closure levels.

The first two test types were constant stress ratio
tests. The first test type was the proposed ASTM standard load
shedding test described previously (Figure 1a). This test
produces a decreasing plastic zone until threshold crack
growth is reached. The second constant stress ratio test
consisted of gradually increasing ΔK at a constant stress
ratio on a non-propagating specimen (see Figure 1b). After
each increase in ΔK, a number of cycles were applied to the
specimen to insure there was no crack growth. When crack
growth was detected above the threshold level, the crack was
grown at a constant maximum load and constant stress ratio to
measure crack growth rate near and beyond the threshold
region. These two constant stress ratio tests were conducted
in a previous study by Jira et al. (3:1-10). The results of
these tests will be referred to as the 'reference tests' later
in this paper.

The second set of tests were constant K_{max} tests. In
contrast to the load shedding test, this test maintains a
constant plastic zone size at the crack tip during crack
growth. The first constant K_{max} test consisted of linearly

4

increasing the minimum stress intensity (K_{min}) of a specimen with a propagating crack until threshold is reached (see Figure 2a). For the second constant K_{max} test, K_{min} is decreased on a specimen which had a non-propagating crack (see Figure 2b). After each decrease in K_{min} a number of cycles was applied to the specimen to insure the crack was not growing above the threshold level. When threshold crack growth was first detected, the crack was grown at a constant maximum load and constant stress ratio to measure crack growth rate near and beyond the threshold region.

All experiments were conducted under fully automated computer control using a laser interferometric displacement gage (IDG) to measure crack growth and closure load.

a. CONSTANT KMAX INCREASING KMIN

b. CONSTANT KMAX DECREASING KMIN
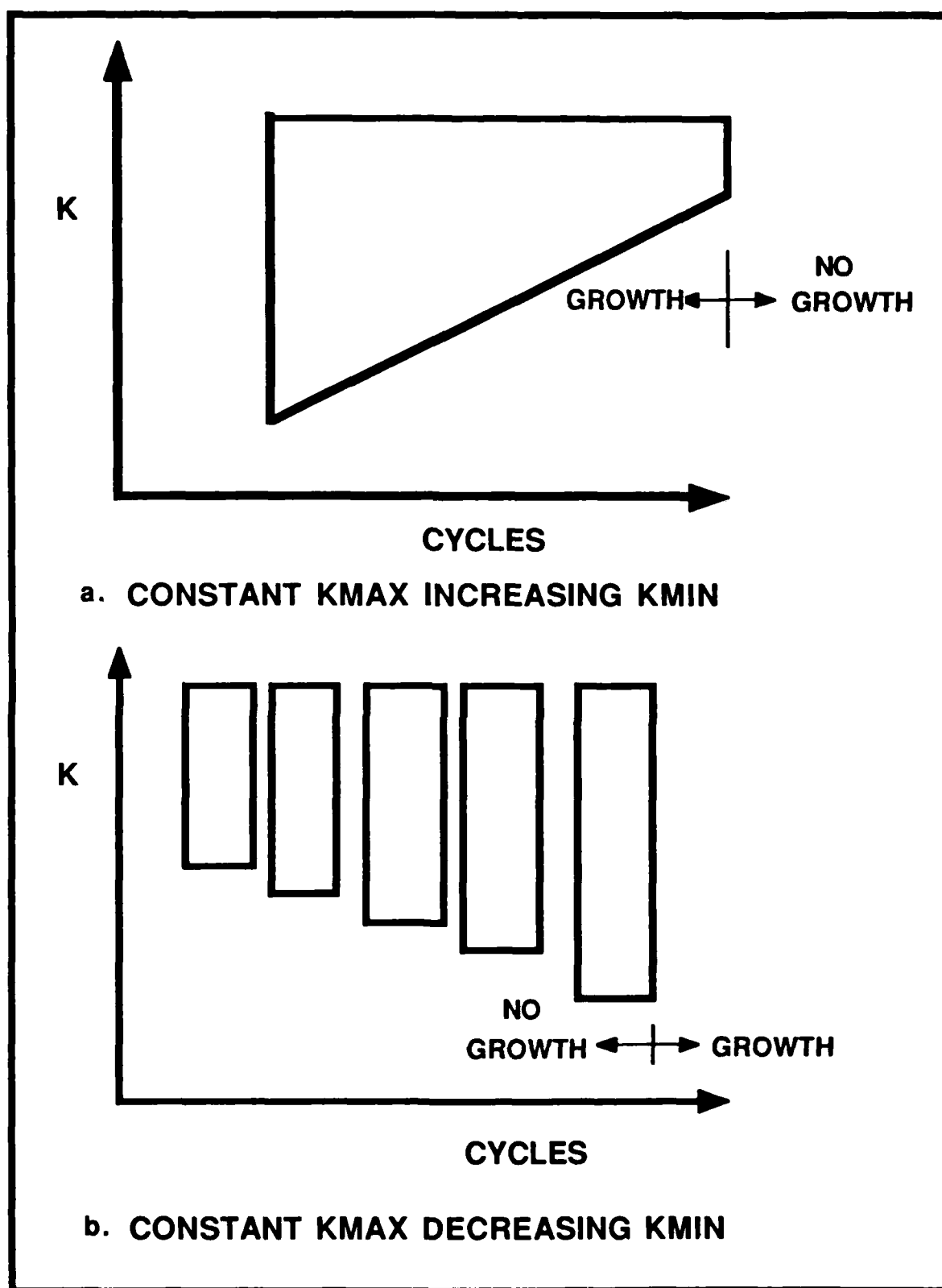
Figure 2. Constant K_{max} Tests

6

II. History-Background

Recently, there has been a great deal of research activity in the field of fracture mechanics, in an attempt to develop a procedure to accurately predict the life of materials subjected to near-threshold fatigue crack growth. These studies have concentrated on closure effects for fatigue crack growth and stress intensity factor measurement techniques for materials.

Crack Growth Prediction

The life expectancy of a structure experiencing fatigue crack growth is governed by the Paris-Erdogan (4:528,534) equation:

$$da/dN = A \, \Delta K^n \qquad (2)$$

where da/dN is crack growth rate, ΔK is stress intensity factor range ($K_{max} - K_{min}$), and A and n are material properties. If A and n can be determined from a test specimen, the component life, N, can be calculated.

Equation 2 is valid for any crack size or specimen geometry. It is not valid if the stress ratio, R, differs from the test specimen, the crack length of the component is short, or the component experiences variations in the load sequence which leads to load interaction and crack growth retardation or acceleration.

Another limitation of Eqn (2) is that it can only be used to model crack growth on the linear portion of the typical fatigue crack growth curve (Figure 3). Since a large portion of a material component's life may be spent in the

7
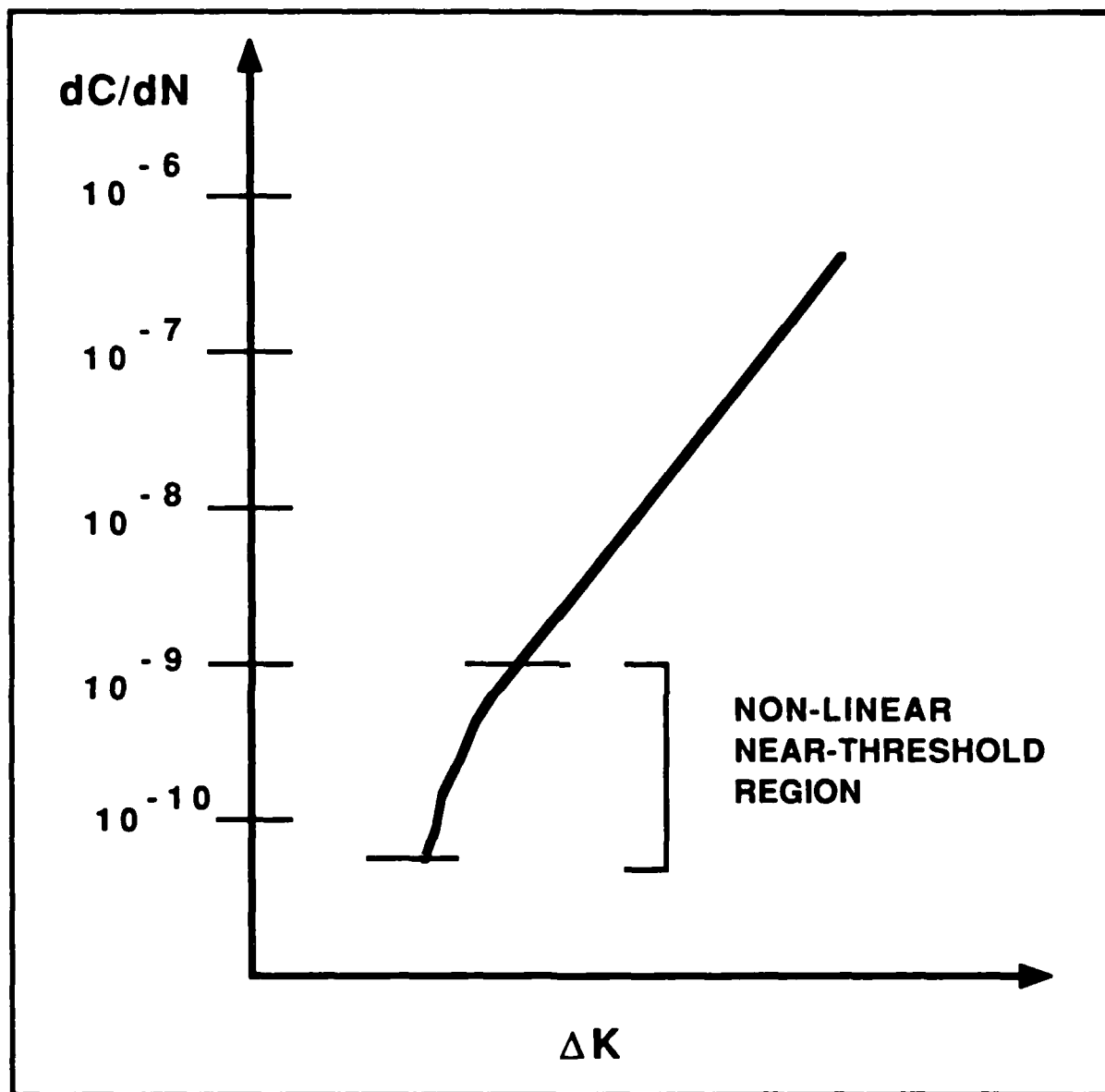
Figure 3. Typical Fatigue Crack Growth Curve

near-threshold, non-linear portion of this curve, it is
essential that Eqn (2) be modified to accurately model this
area.

Closure

To account for the limitations of Eqn (2), Elber
(5:37-45) was the first to propose the concepts of closure and
effective stress intensity factor, ΔK_{eff}. Closure is the
premature contact of a crack's fracture surfaces during a
fatigue cycle. The three primary closure producing mechanisms
are fracture surface plasticity (5:40), oxides (6:293-299),
and fracture surface roughness (7:135-148). These can occur
together or act separately. A knowledge of the closure
producing mechanisms is essential to accurately predict
closure levels, crack growth rates, and component fatigue
life.

Fracture surface plasticity was first addressed by Elber
(8:230-242). Elber proposed that a zone of residual tensile
deformation is formed during fatigue crack propagation. This
zone is commonly referred to as a 'plastic wake' since it forms
in the wake of the plastic zone traveling with the crack tip
(Figure 4). When there is no external load on the specimen,
the material in the plastic wake remains extended and can no
longer be accommodated within the surrounding elastic field.
This produces compressive stresses over the plastic wake. As a
result, when the specimen is unloading, normal compressive
stresses act over the two crack surfaces keeping them pressed
together.

9
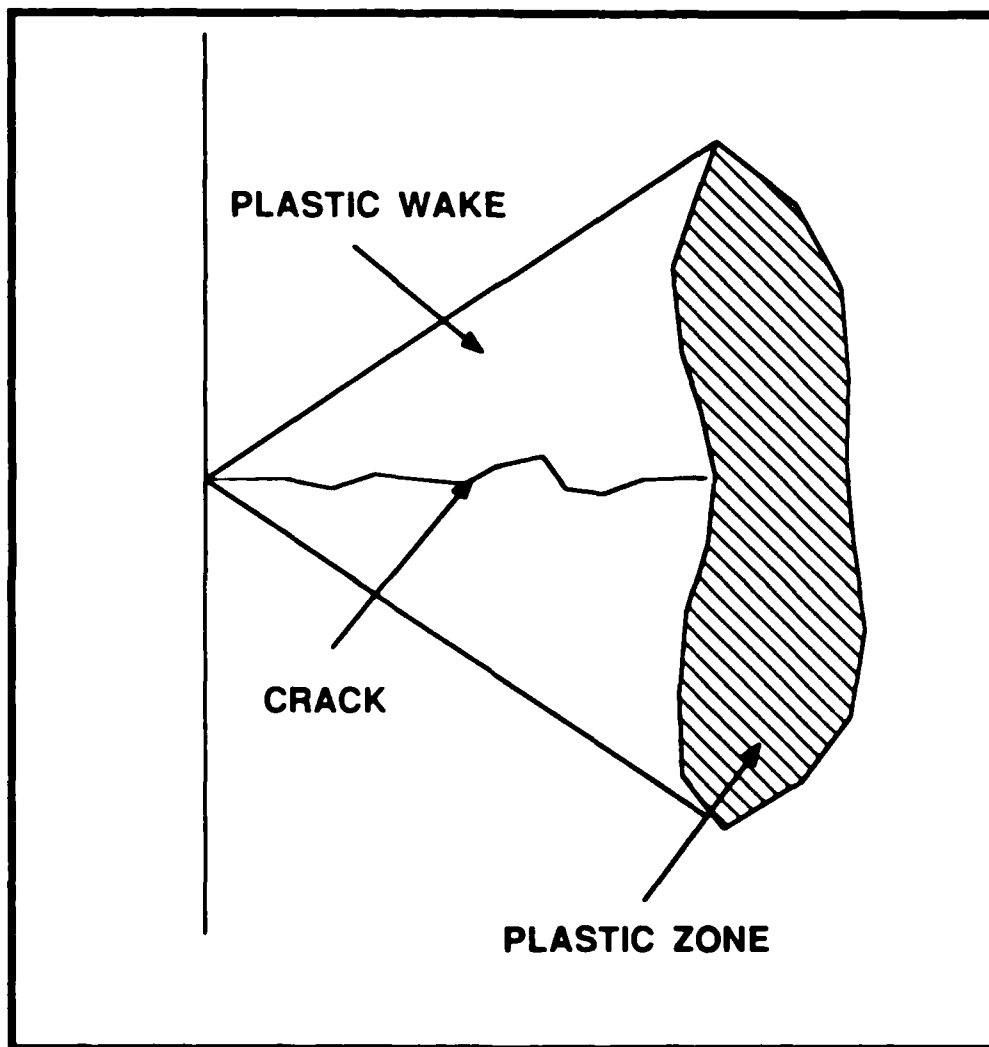
Figure 4. Plastic Zone during Fatigue Crack Growth

The plastic wake results from the formation of a monotonic plastic zone ahead of the crack front during the tensile phase of cyclic loading. This monotonic plastic zone grows along with the fatigue crack. During unloading the monotonic plastic zone experiences compressive stresses as the elastic stresses acting over the crack surface close the crack. This results in yielding in compression over that area where compressive stress exceeds the yield strength. The effected area is referred to as a cyclic or reverse plastic zone and the process is called reverse plasticity.

Oxide induced closure is the second common closure mechanism. It results when a propagating crack experiences surface oxidation and corrosion products build up near the crack tip. These corrosion products can have a thickness several microns thick and wedge-open the crack during the unloading portion of the cycle. This causes premature contact of the crack surfaces, increasing closure loads and decreasing ΔK_{eff}. Oxide induced closure is commonly found at low growth rates ($< 10^{-6}$ mm/cycle).(9:41-45)

The present study's tests were conducted at high cycle (20 hertz) in a non-corrosive environment which reduces oxide formation, therefore oxide induced closure is not considered a significant factor for these tests.

The final closure mechanism is roughness-induced closure. It is common in materials where the maximum plastic zone size is less than the order of grain size, the reverse plastic zone becomes of the order of the grain size, or

11

fracture surface roughness is comparable in size scale with the crack tip opening displacement. The asperities on the crack surface interfere and prevent the crack from closing. This wedging action is localized at a point right behind the crack tip. As with oxide induced closure, asperity induced closure is most common during near-threshold crack growth (9:27-29).

Crack deflection is another mechanism of asperity closure. If the crack does not grow linearly because of load excursions or the microstructure of the material, there is a reduction in the local driving force. This non-linear crack appears to grow slower than a linear crack and therefore results in lower than actual computed crack growth rate (1:238). Crack deflection is a very prominent closure mechanism for the material used in these tests.

The three roughness-induced closure models are (9:30-40):

    1. Single Asperity Model

    2. Spring Clip Model

    3. Fracture Surface Roughness Model

Recent studies (11:20-25) of fatigue crack growth in Ti-Al alloys have shown that the asperity heights were in the range of hundreds of microns. This shows that asperity-induced closure should be a factor for these tests.

In conclusion, fracture surface plasticity, roughness-induced closure, and crack deflection are the prominent closure mechanisms for the material used in this test.

Surface Flaw Closure

Determining closure for a surface flaw fatigue crack, as used in this experiment, is difficult. At the surface the crack is subject to plane stress while in the interior the crack experiences plane strain. The surface crack may change shape while propagating and the growth rate may differ from the surface to the interior. Plasticity closure is more evident at the surface of the crack than in the interior (9:116).

Experimental measurements of closure for surface cracks were conducted using a push-rod gage at the interior and strain gages at the surface of the crack (12:225-239). The results showed $U_{interior}/U_{surface} \sim 1.13$, where U is defined as:

$$U = \frac{K_{max} - K_{op}}{K_{max} - K_{min}} = 0.5 + 0.4 \, R \qquad (3)$$

This shows that the closure is stronger at the surface than in the interior. Another experiment estimated $U_{interior}/U_{surface}$ using crack growth rate, K_{op} at the crack's surface, and the observed aspect ratio changes of the crack as it grew (13:215-218). The results obtained were very close to the previous experiment. These results were used in a subsequent experiment to accurately predict the crack growth rate for a crack subject to a single overload cycle (12:235-239).

It has been suggested that when compliance is used for computing crack growth rates of surface flaws the measurement technique should be able to determine small displacements

13

right at the opening of the surface flaw and account for shape change (aspect ratio) effects on compliance (14:66). The interferometer displacement gage used to measure crack mouth opening displacement (CMOD) for these tests can measure small displacements at the crack tip. The Raju-Newman equations used to calculate the stress intensity of the elliptical cracks in this test do account for variations in aspect ratio.

In another study, Prodan and Erismann (15:1927-1934) compared stress intensity factors obtained from a standard (CT) specimen to those from proposed stress intensity factors obtained for an elliptical surface flaw, using the methods proposed by Newman and Raju (16:817) and Irwin (17:651). Prodan and Erismann found that the ΔK values obtained for the surface flaws were very similar to those obtained for the CT specimen. They concluded that the experimental results obtained from CT specimen testing can be applied to surface flaw fatigue growth predictions with good conservative results. Other researchers did not feel that CT crack growth data should be compared to surface flaw data since the surface flaw has such significant changes in shape and variations in stress (14:60). There is a general consensus that the Raju-Newman stress intensity formulas for surface flaws is accurate for crack growth predictions (14:60). The Raju-Newman stress formulas were used for the tests conducted in this study.

Stress Intensity Factor

Once closure is accurately calculated, prediction of

stress intensity factor, K, and component life can be made. Crack closure decreases the applied stress intensity factor ($\Delta K = K_{max} - K_{min}$) at the crack tip. The actual stress intensity at the crack tip is defined as effective stress intensity, $\Delta K_{eff} = K_{max} - K_{cl}$. K_{cl} is the closure stress intensity factor.

The threshold stress intensity factor, ΔK_{th}, is defined as the stress intensity factor below which the crack will not propagate. The threshold crack growth rate is generally accepted as 10^{-10} m/cycle. The time required to experimentally determine crack growth below this level makes it impractical.

Effective Threshold Stress Intensity Factor

The ASTM recommended method for determining ΔK_{th} (1:248) is to initiate crack growth at a high ΔK. ΔK is then gradually decreased with crack growth until the threshold crack growth rate is obtained. This test is run under fully automated computer control in accordance with the following equation:

$$K = K_o \exp [C (a - a_o)] \qquad (4)$$

K is the present stress intensity factor, K_o is the initial stress intensity factor, a is the present crack length, a_o is the initial crack length, and C is a constant which determines how quickly ΔK is decreased.

A critical consideration is to ensure that the crack grows beyond the plastic zone induced by the previous loading. The ASTM proposed method gives the minimum crack advance, Δa, between load decrements at the ith step down should be (2:59-75):

15

$$\Delta a > 0.5 \text{ mm}$$

$$1/K * dK/da < -0.08 \text{ mm}^{-1}$$

The stress intensity factor threshold values obtained from these tests have varied as much as 40% at low stress ratios (R) (2:66). Cadman et al. (2:67-68) conducted load shedding tests for a 0.15%C, 1.5%Mn steel alloy used in construction engineering. The testing was conducted on a resonant-frequency electro-magnetic fatigue machine, measuring crack growth by the direct current potential method. They found ΔK_{th} values as much as 40% less than values obtained from an earlier test (10:151-158) at low values of R. They found good agreement at high values of R. Cadman et al. have suggested fatigue thresholds measured from decreasing ΔK tests should be specified in terms of the ΔK reduction rate. He found significant differences in ΔK_{th} with ΔK reduction rate and test loading frequency. He also recommended that the published threshold values are only relevant to the specific stress history of the test and should not be considered a material property. This demonstrates the sensitivity of near-threshold crack growth rate measurements to loading history, closure loads, and plastic zone.

Döker et al. (18:50-51) conducted load shedding tests on a commercial Ti-6Al-4V alloy using a load controlled servohydraulic testing machine. Crack growth was measured using the potential drop method. Döker et al. found that ΔK_{th} varied exclusively with R. He expressed the opinion that ΔK_{effth} values obtained from decreasing ΔK tests for low R

16

values should not be viewed as a material property because of the difficulty in obtaining closure values. Döker et al. did feel that it was possible to establish a characteristic crack growth curve in the near-threshold regime using ΔK_{eff}. This testing points out the possibility that a constant ΔK_{effth} value is obtainable if closure can be accurately measured at low R.

Jira et al. (3:6) found that the ΔK_{th} values obtained for a high strength titanium alloy, Ti-6Al-2Sn-4Zr-6Mo, varied with the amount of closure present in precracking. They were, however, able to get similar ΔK_{th} values and near-threshold crack growth rates from different R ratios using ΔK_{eff} obtained through closure measurements (Figure 5). There was no closure at R = 0.5, therefore the crack growth curve did not change when plotted versus ΔK_{eff}. This consolidation of crack closure thresholds and near-threshold crack growth rates using ΔK_{eff} was demonstrated for both long and short crack data from increasing and decreasing ΔK, constant K_{max} tests (see Figures 1a and 1b). Jira observed that there appeared to be a single crack growth rate curve and threshold value (ΔK_{effth}) when ΔK_{eff} is used to correlate the data. These results point to the possibility that ΔK_{effth} could be the material property needed to modify the Paris-Erdogen equation for near-threshold crack growth.

Using the above data, Eqn (2) can be rewritten:

$$da/dN = A \, \Delta K_{eff}^{n} \tag{5}$$

This appears to be valid for most 'long' cracks. Long cracks
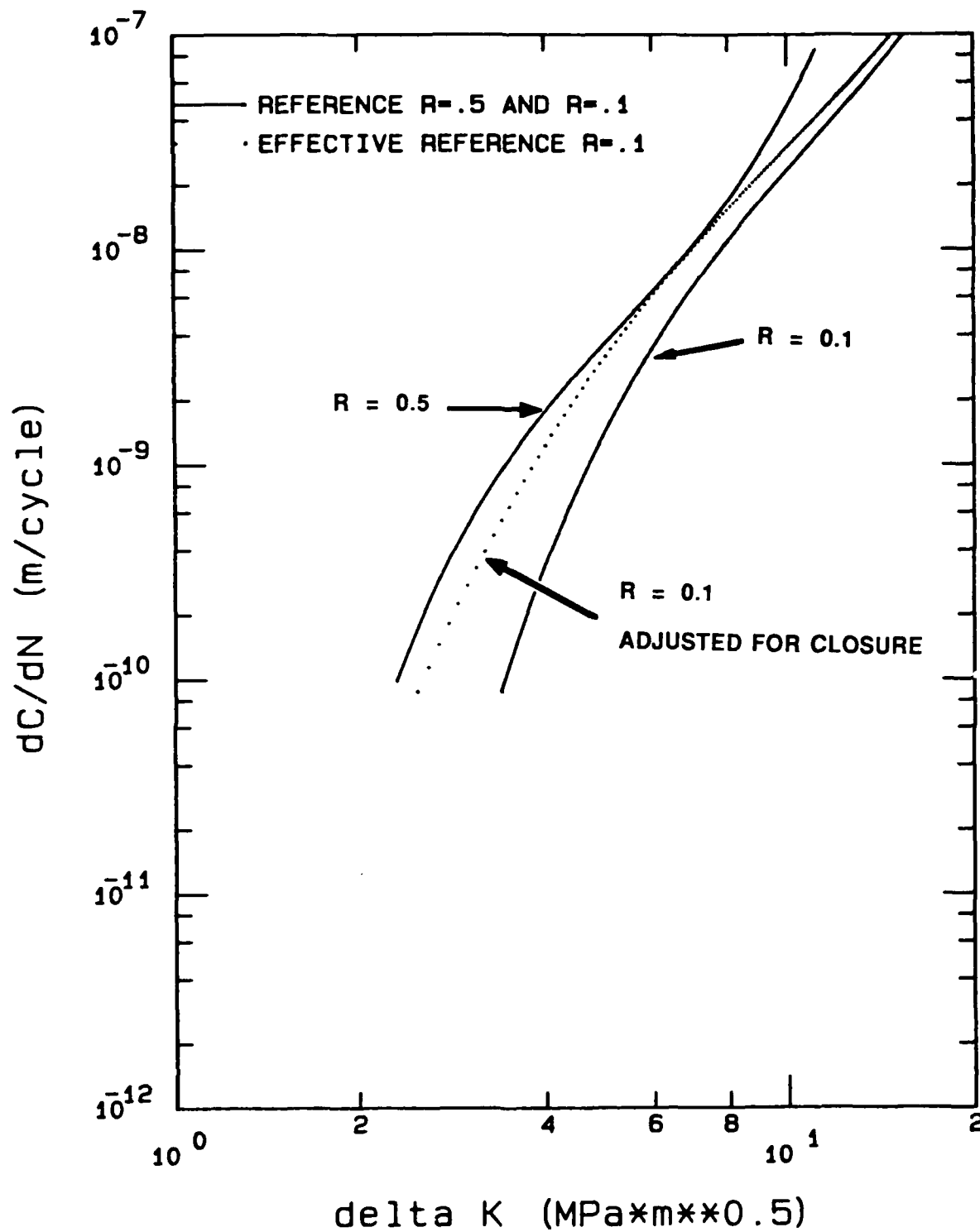
17

Figure 5. Crack Growth Curves With and Without Closure Effect

18

are described as those cracks which are much longer than the crack tip plastic zone as is true for the cracks examined in these tests.

While Jira et al. was able to consolidate crack growth rate using ΔK_{th}, others tried new test types to gage the effects of closure and loading history on crack growth predictions. Herman et al. (19:32) conducted ΔK threshold tests on low carbon Astroloy, a hot isostatically pressed Nickel-based superalloy, 2024-T3 wrought aluminum and extruded 6005 aluminum alloys. The tests included a constant R (0.1) decreasing ΔK threshold test, and a constant K_{max} increasing K_{min} test. Herman concluded that the conventional decreasing ΔK threshold tests produced nonconservative values of ΔK_{th}. His recommendation was to use the constant K_{max} increasing K_{min} test results for predicting the life of components with large amounts of closure. He also concluded that the decreasing ΔK tests should only be used at high R ratios. One aspect of the constant K_{max}, decreasing K_{min} test is that the plastic zone remains constant during the entire test. This allows large ΔK reduction gradients without effecting threshold results. The constant K_{max} test also provided crack growth rate results from large cracks which compared favorably with short crack growth rate results from previous tests.

The results obtained by Jira et al. show a possibility that ΔK_{effth} could be used as a material property to modify the Paris-Erdogen equation to predict near-threshold crack growth. however, there is a need to examine how ΔK_{effth} would

19

vary under different loading conditions and closure loads, from the proposed ASTM standard load shedding test used by Jira et al. If ΔK_{effth} is indeed a material property, its value would not change with a different loading history. Hence this study was undertaken to investigate the effect of these factors on threshold fatigue crack growth behavior.

III. Testing Procedure

Specimen Preparation

Testing was conducted on the alloy Ti-6Al-2Sn-4Zr-6Mo. A complete chemical breakdown is presented in Table I. This material was selected since it is frequently used in high performance gas turbine engines where fracture mechanics is employed to predict the life expectancy of structures with small cracks.

The material was cast and isothermally forged at 913°C into circular disks approximately 50 mm thick and 500 mm in diameter. The material was heat treated at 921°C for two hours, fan air cooled; heated to 824°C for two hours then water quenched; heated to 593°C for eight hours then air cooled. The material had a yield strength of 1158 MPa and ultimate strength of 1230 MPa. It was essentially isentropic.

The dimensions of the specimen are shown in Figure 6. The gage sections of the specimens were electropolished to a minimum depth of 0.2 mm to eliminate surface residual stresses and roughness produced during machining. The electropolishing had the additional benefit of supplying a highly reflective surface for optical crack measurement while highlighting the specimen's microstructure. A semicircular electro-discharge (EDM) notch, approximately 250 μm wide and 80 μm high and 125 μm deep, was machined on each specimen for crack initiation. Vickers hardness indents were placed on opposite sides of the EDM notch for crack opening displacement (COD) measurements

21

Table I. Chemical Composition of Ti-6Al-2Sn-4Zr-6Mo

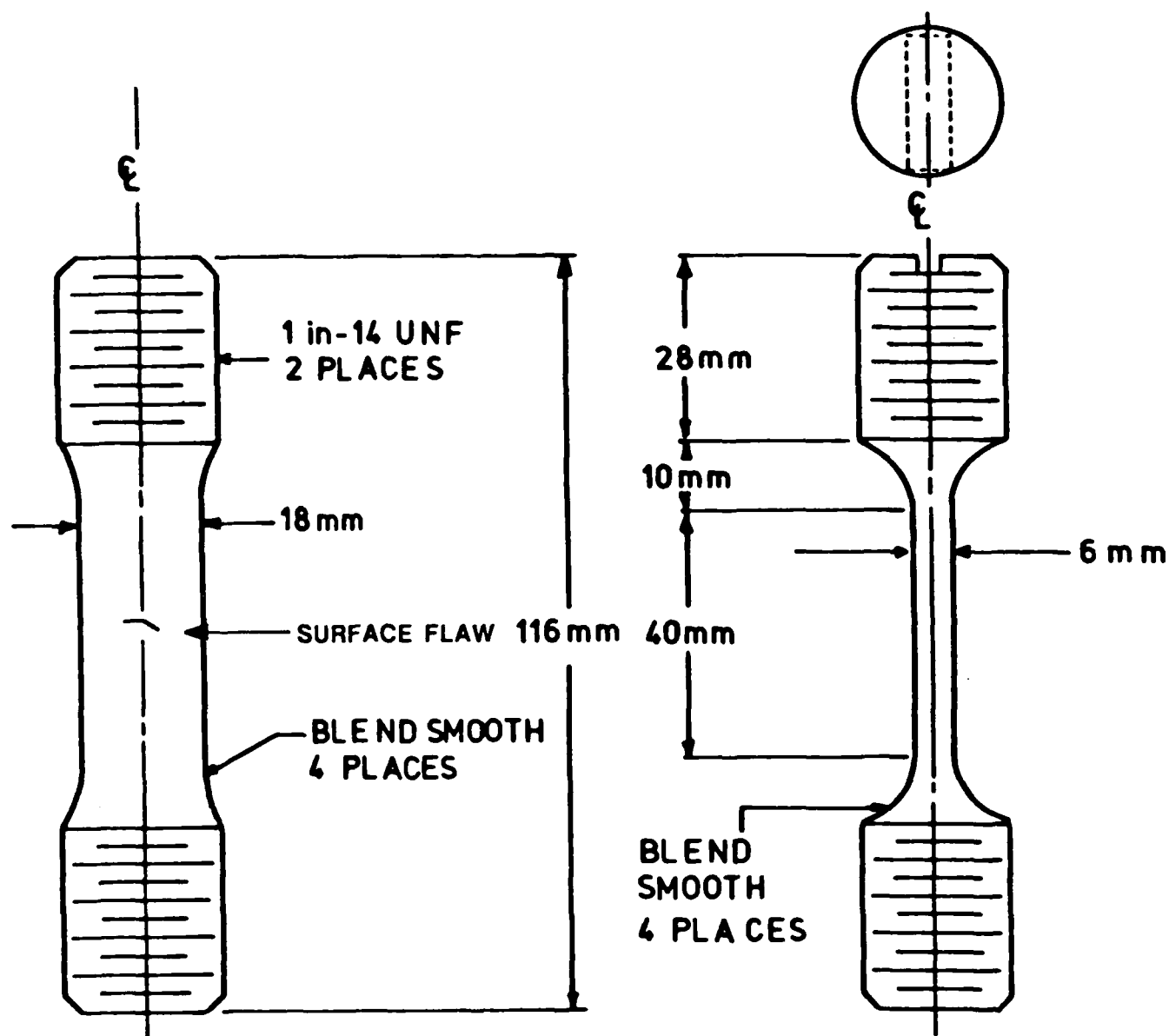| ELEMENT	WEIGHT PERCENT
Al	6.33
B	0.01
C	0.02
Cu	0.01
Fe	0.12
H	0.0017
Mo	5.76
Zr	3.93
N	0.01
O	0.10
Si	0.09
Sn	2.07
Ti	Remainder
Y	0.0010

Figure 6.   Specimen Configuration

23

using a laser interferometer displacement gage (IDG). The IDG is detailed in the Test Set-up section.

All specimens were precracked to ensure there was no residual stress effects from the EDM notching. The crack was initiated and grown a distance equal to the radius of the notch (0.1 mm) to ensure a proper starter crack. The precracking was accomplished using a constant maximum load and constant stress ratio, R, $(\sigma_{min}/\sigma_{max})$. All precracking was done at a frequency of 10 hertz. All specimens were precracked with R = -1.0 to maintain a constant loading history. The maximum stress for precracking varied between 0.2 σ_{ys} and 0.3 σ_{ys} (σ_{ys} = 1158 MPa). The selected precracking maximum load was chosen so it would not exceed the initial maximum load of the test and induce an overload condition. One specimen did not develop a crack at an R of -1.0, because of a particularly blunt notch. This specimen was initially precracked at an R of -1.5 until the crack developed. Once the crack started to grow the the load ratio was reduced to -1.0 during the remainder of the precracking.

A complete summary of all tests is presented in Table II.

24

SPECIMEN	TEST TYPE	PURPOSE	PRECRACKING DETAILS	INITIAL CONDITIONS	FINAL CONDITIONS	REMARKS
86002	CONSTANT K_{max} INCREASING K_{min}	THRESHOLD TEST	R = -1.0 P_{max} = 24Kn	R = 0.1 P_{max} = 28Kn	R = 0.6 P_{max} = 18Kn	K_{max} = 6
	CONSTANT P_{max} CONSTANT R	GROWTH RATE TEST	N/A	R = 0.6 P_{max} = 18Kn	R = 0.6 P_{max} = 18Kn	
86003	CONSTANT K_{max} INCREASING K_{min}	THRESHOLD TEST	R = -1.0 P_{max} = 22Kn	R = -0.3 P_{max} = 38Kn	R = 0.44 P_{max} = 9Kn	K_{max} = 4
	CONSTANT P_{max} CONSTANT R	GROWTH RATE TEST	N/A	R = 0.44 P_{max} = 9Kn	R = 0.44 P_{max} = 9Kn	
86010	CONSTANT K_{max} DECREASING K_{min}	THRESHOLD TEST	R = -1.0 P_{max} = 30Kn	R = 0.7 P_{max} = 36Kn	R = 0.58 P_{max} = 36Kn	K_{max} = 6
	CONSTANT P_{max} CONSTANT R	GROWTH RATE TEST	N/A	R = 0.58 P_{max} = 36Kn	R = 0.58 P_{max} = 36Kn	
86020	CONSTANT K_{max} DECREASING K_{min}	THRESHOLD TEST	R = -1.0 P_{max} = 22Kn	R = 0.42 P_{max} = 28Kn	R = 0.21 P_{max} = 28Kn	K_{max} = 4
	CONSTANT P_{max} CONSTANT R	GROWTH RATE TEST	N/A	R = 0.21 P_{max} = 28Kn	R = 0.21 P_{max} = 28Kn	

Table 11. Summary of Test Plan

Test Set-Up

All tests were run on an MTS machine at room temperature (23°C) under a fully automated computer controlled mode. A laser interferometer displacement gage (IDG) was used to get accurate measurements of crack lengths and near crack tip surface closure loads. The system is diagrammed in Figure 7.

The IDG measures the relative displacement between the two Vickers hardness indents. The indents form two interference fringe patterns from overlapping diffracted laser beams. The motion of the fringe pattern is recorded on linear arrays made from 1024 detector elements placed 13 microns apart along a 13.3 mm long axis. A sequential scan of this array produces a digital representation of the fringe pattern. The system can then monitor the fringe pattern as a function of time, using an IBM 9000 Microcomputer. The system, developed by Sharpe (20:1-10) and modified by Hartman (21:1-9), provides a displacement resolution of approximately 2.0 μm.

This system produced load-crack mouth opening displacement (CMOD) curves at selected intervals during the test which were used to determine both crack length and closure loads. Crack length was calculated from the elastic compliance determined from the slope of a straight line fitted to the linear portion of the curve. The compliance for this specimen with the same type of crack length was established in previous studies (22:201-212). Closure load was measured using the intersection method. The intersection method fits a
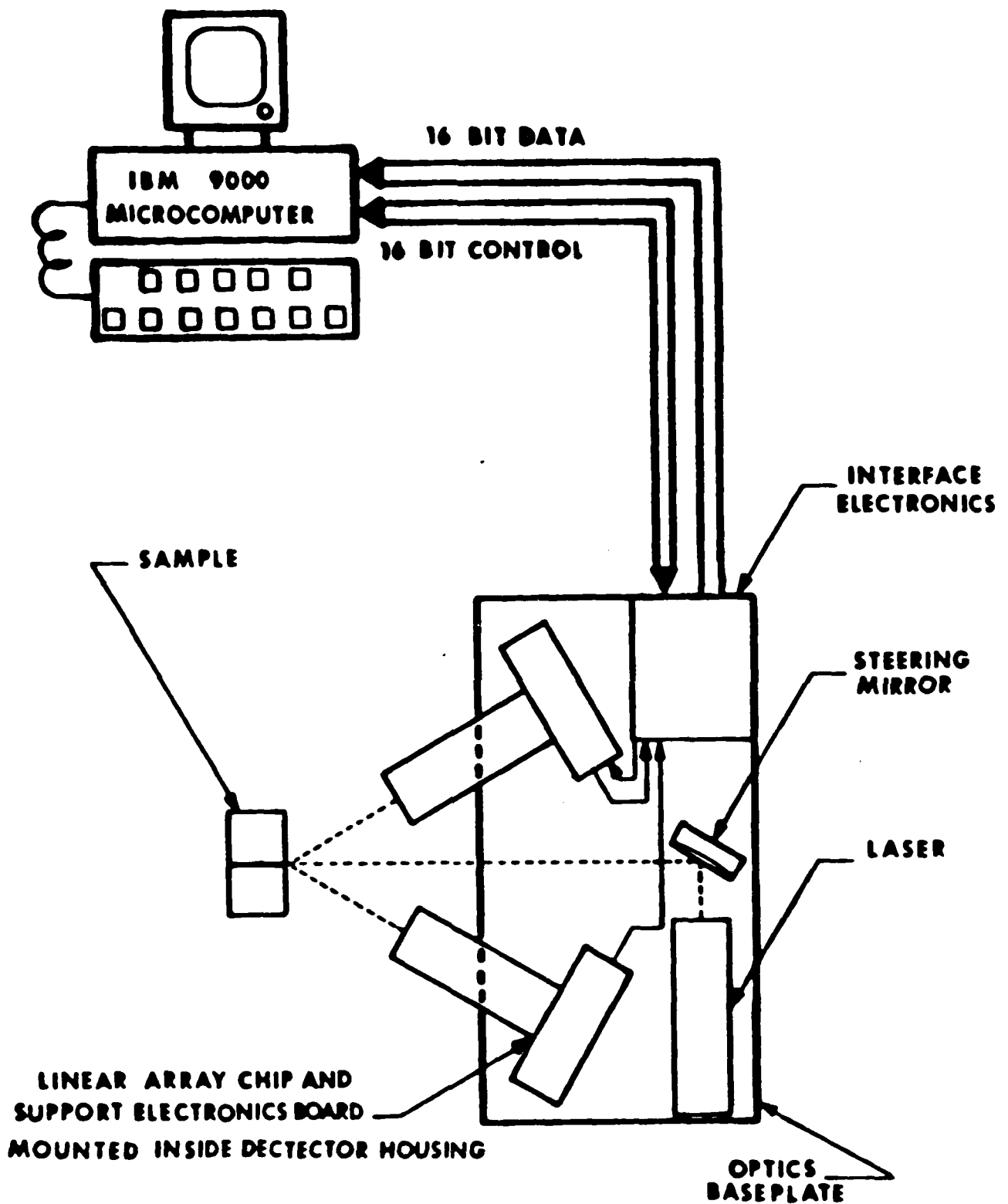
26

Figure 7.   Test Set-up

27

straight line to the linear portion of the load-CMOD curve and
another line tangent to the non-linear portion of the curve.
The closure load was taken where the two lines intersected. An
example of this is shown on Figure 8. To backup the IDG crack
length measurements, optical measurements of the cracks were
made continuously during the tests using a traveling
microscope.

Test Plan

Earlier studies (3:6) were able to measure a fairly
constant ΔK_{effth} value and crack growth behavior for
Ti-6Al-2Sn-4Zr-6Mo using the proposed ASTM test procedures
(constant R) for calculating ΔK_{th} and using ΔK_{eff} as a single
variable to converge their crack growth data obtained from
different load ratios. This study examined the effects of
varying loading histories (constant K_{max}, varying R), closure
loads, and plastic zones on crack growth rates and threshold
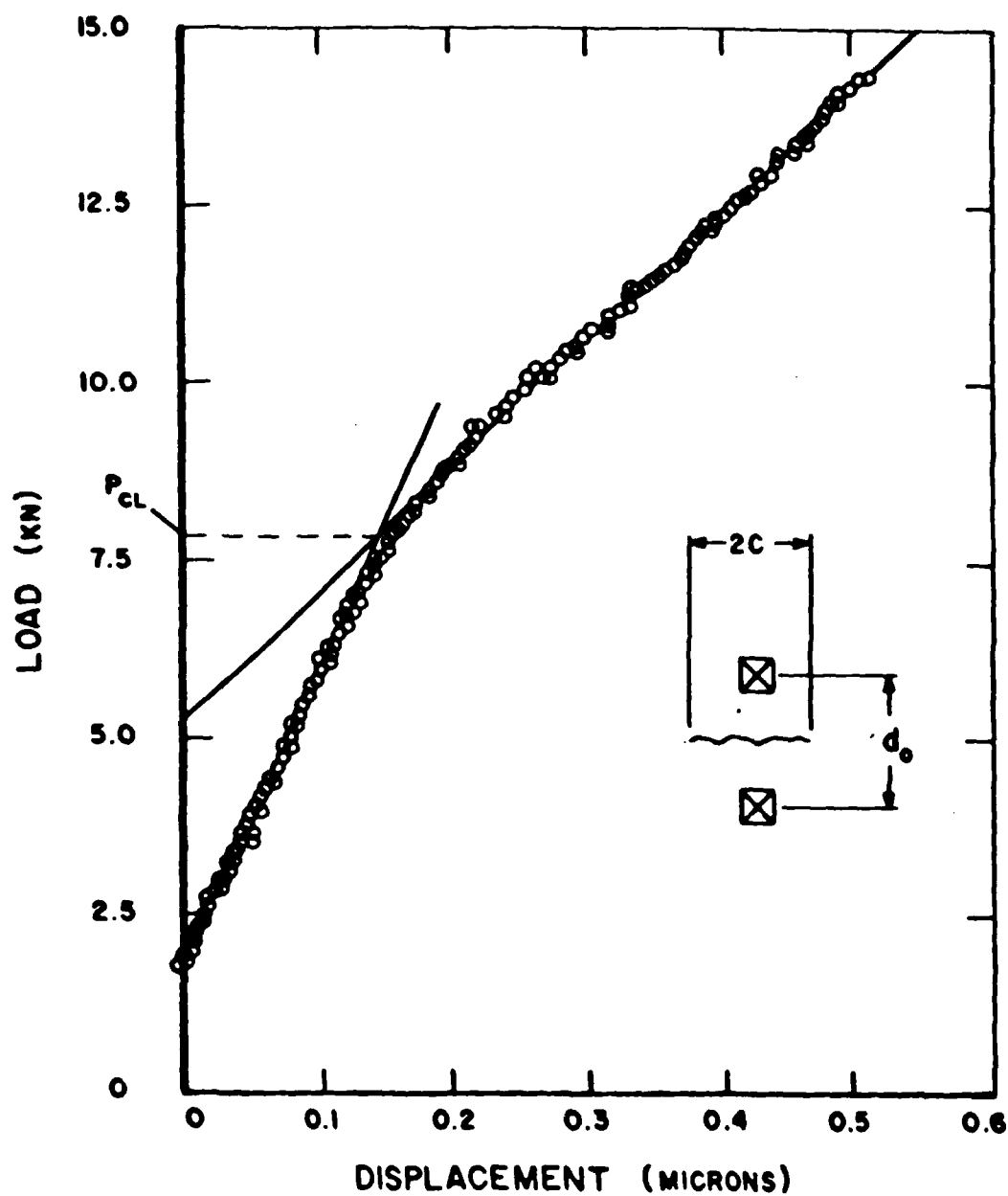stress intensities, by performing the various tests discussed
below.

Figure 8. Intersection Crack Closure Measurement

Decreasing ΔK Test

The decreasing ΔK test is commonly referred to as the load shedding test. This test is the proposed ASTM standard test for determining threshold stress intensity, ΔK_{th}. For this test an initial load is applied to the specimen which results in a propagating crack. As the crack grows, the stress intensity (ΔK) is gradually reduced until the threshold crack growth rate (10^{-10} m/cycle) is reached . This test maintained a constant stress ratio, R.Maximum stress intensity factor for the test was controlled using the following equation:

$$K = Ko \exp [C (a - ao)] \qquad (6)$$

Ko = initial stress intensity
ao = initial crack length
a = current crack length
C = -1.0/mm

To examine the effects of different closure loads, three tests were conducted using R ratios of 0.1, 0.65, and 0.8. The tests using the 0.1 and 0.65 stress ratios were conducted in the reference study (3:1-10).
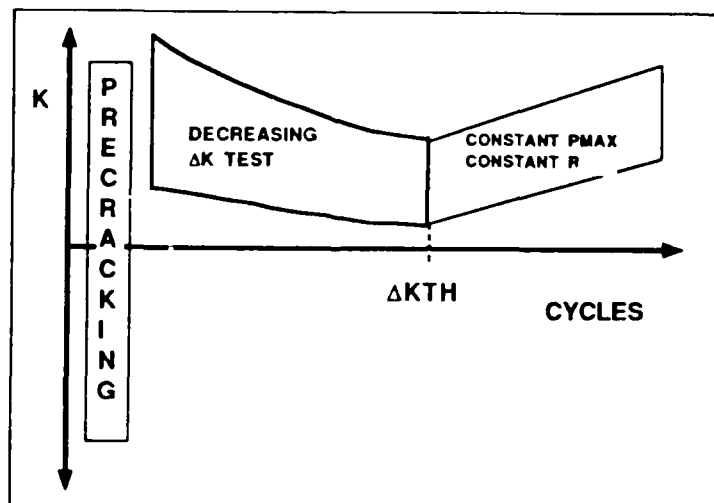

Figure 9. Decreasing ΔK Test

30

Increasing ΔK Test

The second test type was a constant R test. An initial stress intensity (ΔK) was applied to the specimen with a sufficient number of cycles to ensure the crack was not growing more than the rate of $5*10^{-11}$ m/cycle. Once it was determined the crack was not growing, ΔK was increased slightly and a block of cycles was applied to the specimen while the IDG checked for crack growth. The procedure was repeated until crack growth above the threshold rate was detected. After crack growth at the threshold level was detected the crack was grown at a constant load and constant R to measure near-threshold crack growth rate. This test was run at stress ratios of R = .1 and R = 0.65. The values of R were chosen to produce different levels of closure. These tests were conducted in the reference study by Jira et al. (3:1-10).
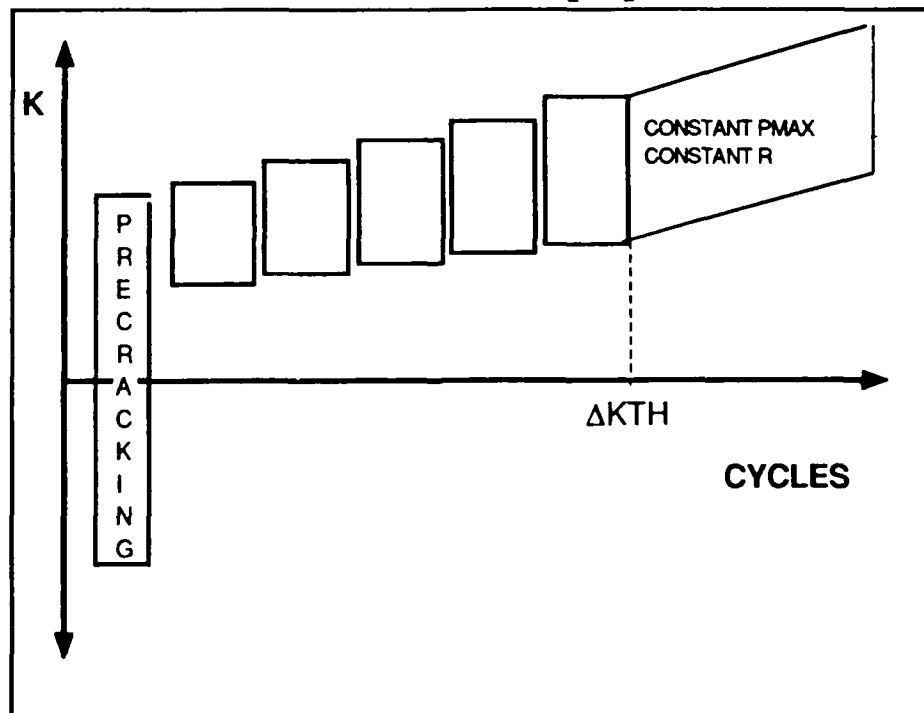

Figure 10.   Increasing ΔK Test

Increasing K_{min} Test

For this test a constant K_{max} is applied to the specimen with a K_{min} which results in a propagating crack. K_{min} is then linearly increased with crack length, through fully automated computer control, until threshold crack growth $(1*10^{-10}$ m/cycle) is obtained. Once threshold crack growth is reached the crack is grown under constant maximum load at the existing R to measure near-threshold growth rate.

This test was run twice at different stress ratios on separate specimens to measure the effects of loading history and different closure loads. During the first test K_{max} was 5.0 MPa√m with an initial R of 0.1. The specimen reached threshold crack growth rate at R = .59.

During the second test K_{max} was 4.0 MPa√m and the initial R was -0.3. Threshold crack growth rate was reached at R = .44. Both tests were run at a frequency of 20 hertz and a room temperature of 23°C.
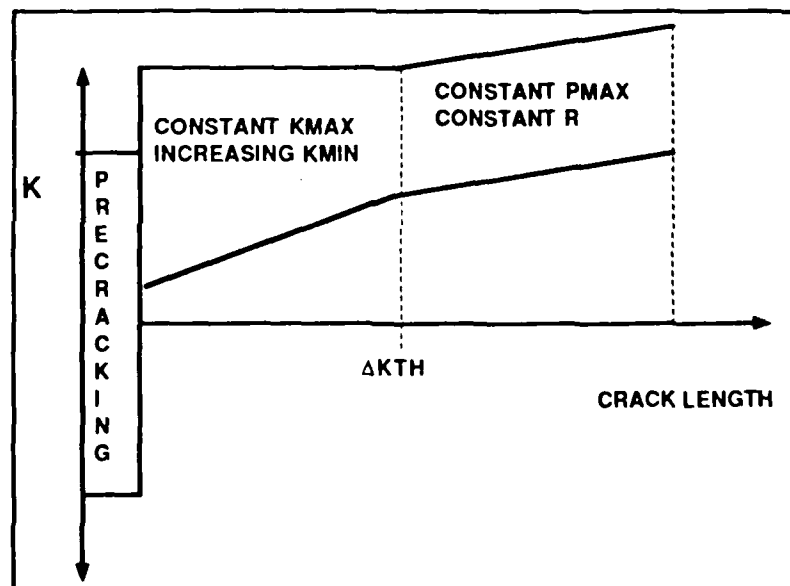

Figure 11.   Increasing K_{min} Test

Decreasing K_{min} Test

This test was a constant K_{max} test. Initially K_{min} was selected to ensure the crack was growing well below the threshold rate. K_{min} was then decreased and a block of 198,000 cycles was applied while the IDG checked for crack propagation. This procedure was repeated until crack growth above the threshold rate ($5*10^{-11}$ m/cycle) was detected. Once threshold crack growth was detected the crack was grown under constant maximum load at the existing R to measure near-threshold crack growth.

This test was run twice at different stress ratios to examine the effects of loading history and different closure loads. The first time this test was run, K_{max} was 6.0 MPa√m and R was initially .70. R was decreased in increments of .02 for each block of cycles. The crack growth rate increased above the threshold rate at R = .64.

The second decreasing K_{min} test was run at K_{max} = 4.0 MPa√m and R was initially 0.4. R was decreased by either .02 or .03 for each block of cycles until the threshold crack growth occured at R = .21. Both of these tests were run at a frequncy of 20 hertz and room temperature of 23°C.
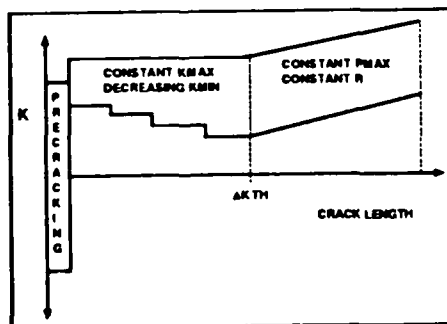

Figure 12. Decreasing K_{min} Test

IV. Results and Discussions

The results for the tests conducted in this study are compared to the results obtained in a previous reference study (3:1-10) using identical material specimens, precracking procedures (R = -1.0), closure measurement techniques (intersection method), and testing apparatus.

The reference study conducted the constant R increasing ΔK and decreasing ΔK tests discussed earlier (Figures 1a and 1b). The results of these tests are contained in Figures 13-16. Figure 13 shows the crack growth rate curves for a typical constant R decreasing ΔK test and a constant R constant P_{max} test. The stress ratio for these two tests was R = 0.1. Figure 14 shows these same crack growth rate curves adjusted for closure load using ΔK_{eff}. The reference R = 0.5 curve is the constant R decreasing ΔK crack growth rate curve of a CT specimen from the same material at R = 0.5. When the crack growth curves are plotted versus ΔK_{eff}, they coincide with the CT specimen's R = 0.5 crack growth rate curve. This coinciding of the crack growth rate curves with the CT specimen's R = 0.5 crack growth rate curve is a typical result of the reference study's tests (3:9). Figures 15 and 16 show the relationship between threshold stress intensity and effective threshold stress intensity for the constant R tests conducted in the reference study (3:10).

The conclusions from the previous study include (3:6):

1. Crack growth rate curves, for different stress ratios, can be consolidated using ΔK_{eff} based on closure

34

measurements in surface flaws in a high strength titanium alloy, Ti-6Al-2Sn-4Zr-6Mo.

2. Both the increasing ΔK and decreasing ΔK threshold tests produced ΔK_{th} values which varied with stress ratio and the amount of closure present. When closure is accounted for, through ΔK_{eff}, there appears to be a single value of effective threshold stress intensity factor, ΔK_{effth}, for all stress ratios.

The purpose of this study is to determine if these results can be duplicated for tests with different loading histories, stress ratios, closure loads, and plastic zones.
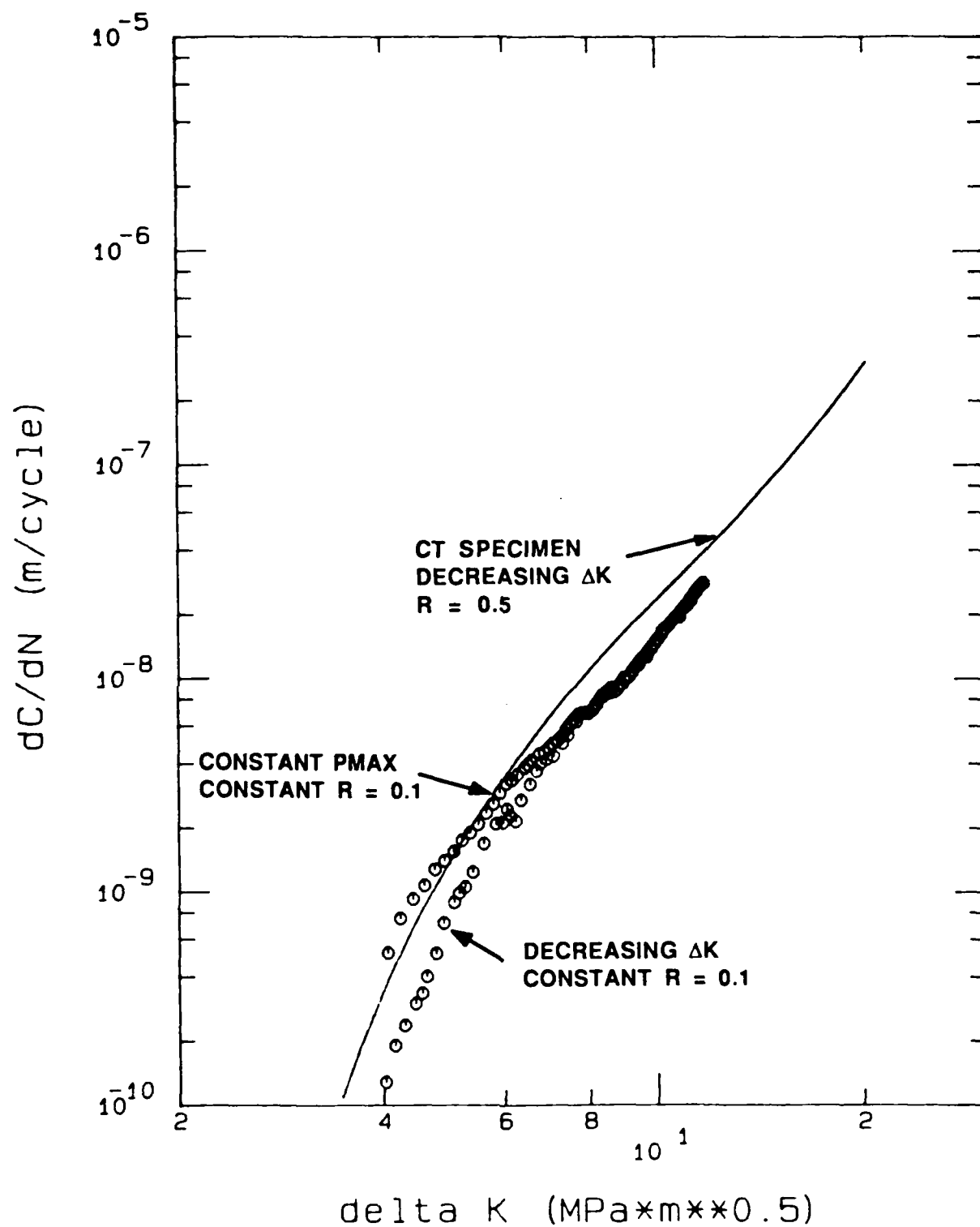
Figure 13. ΔK vs. Crack Growth Rate from Reference
Study Decreasing ΔK Test (3:6)

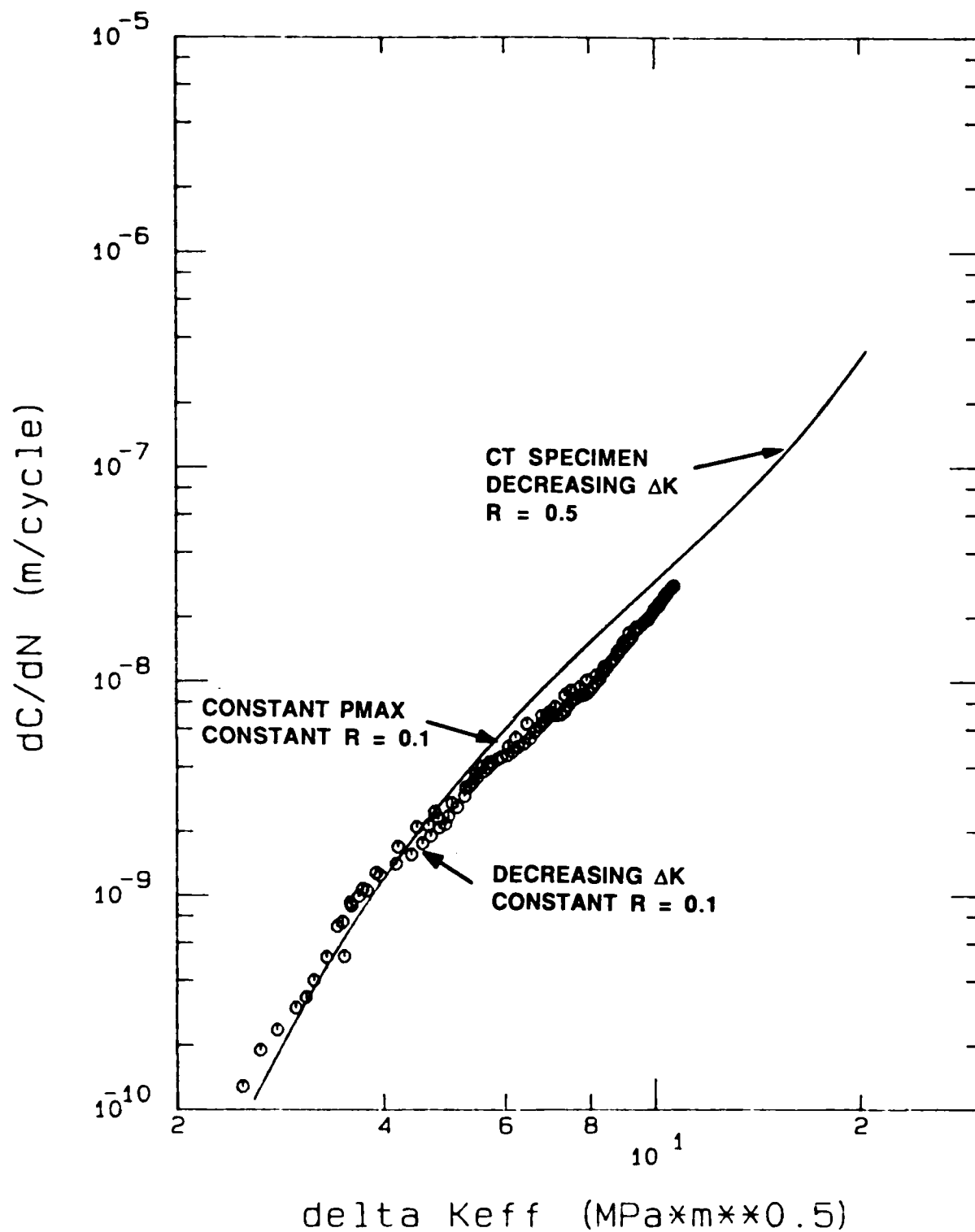Figure 14. ΔK_{eff} vs. Crack Growth Rate from Reference Study Decreasing ΔK Test (3:6)
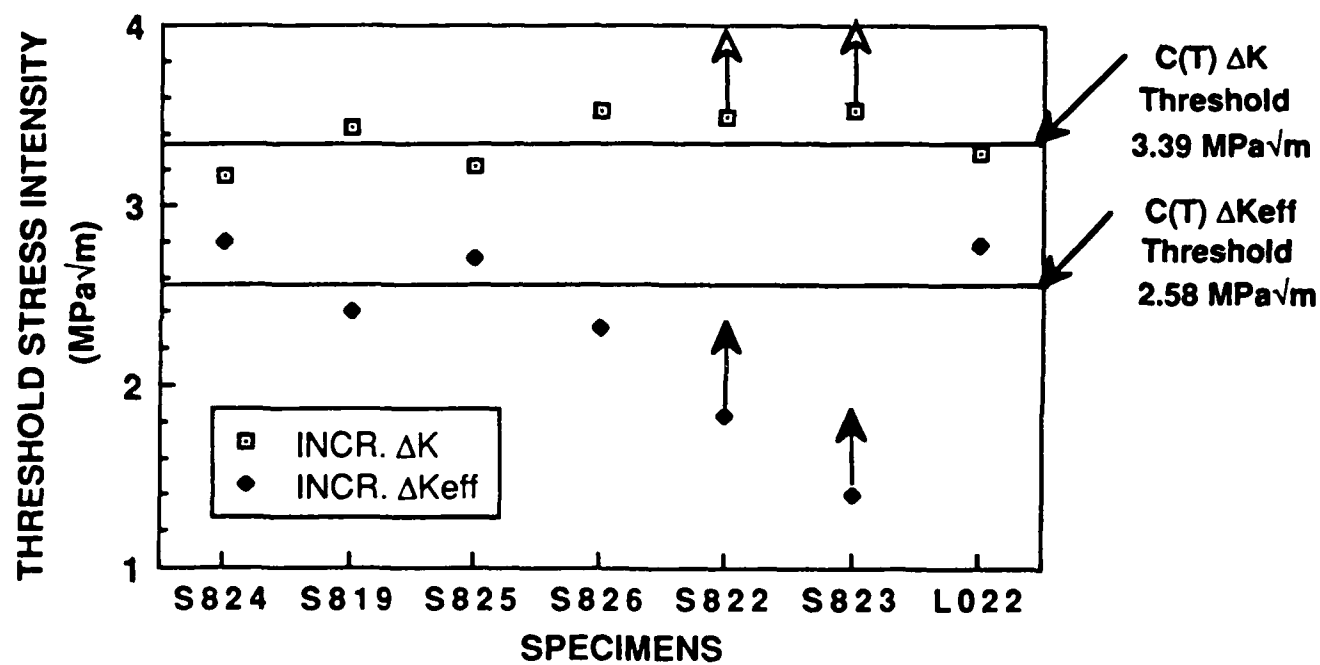
37

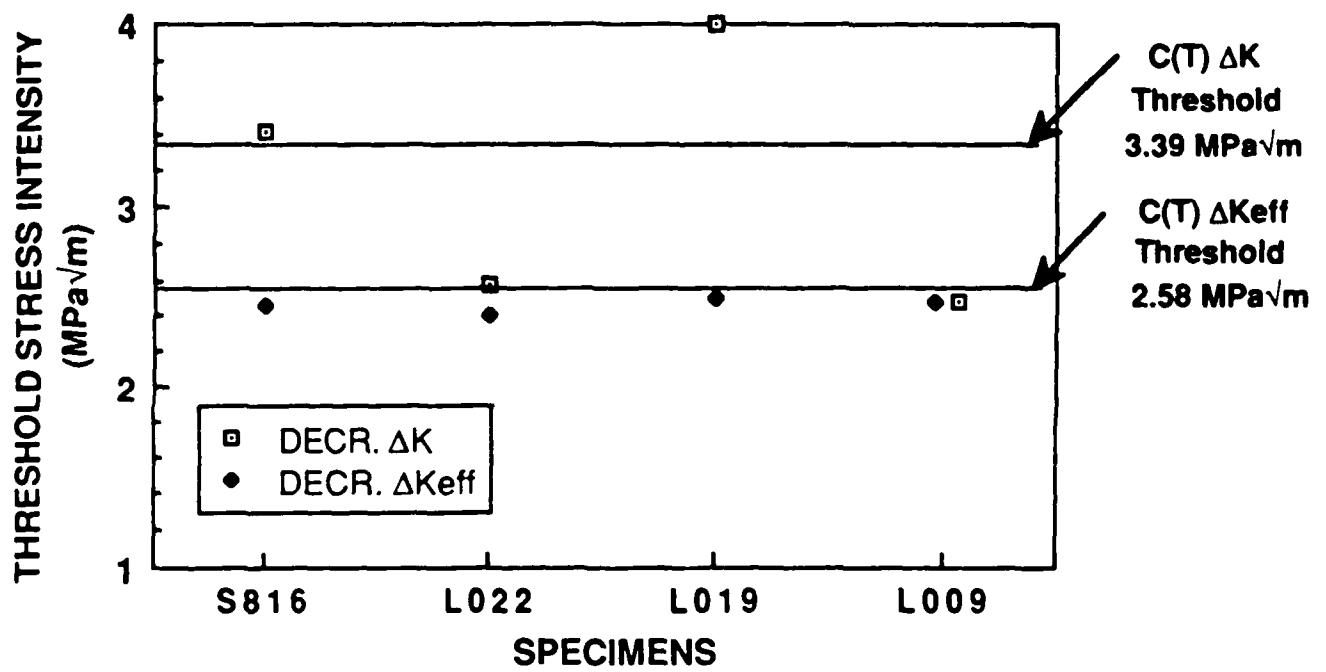Figure 15. Threshold Stress Intensity for Increasing ΔK Tests
(3:10)

Figure 16.   Threshold Stress Intensity for Decreasing ΔK Tests
(3:10)

Constant K~max~ Increasing K~min~ Tests

Specimen 86002 was precracked at a stress ratio of $R = -1.0$. After the starter crack was developed, the constant K_{max} increasing K_{min} test (Figure 11) started at a stress ratio of $R = 0.1$. The threshold crack growth rate ($1*10^{-10}$ m/cycle) was reached at a stress ratio of $R = 0.60$. The resulting threshold stress intensity factor (ΔK_{th}) was 2.44.

The initial stress ratio for this test was low (0.1). This should have produced closure during the start of the test. Closure did develop, even though it can not be seen clearly on Figure 17. As the stress ratio increased, the closure load dropped below the minimum load. The IBM 9000 computer places closure load at minimum load if it sees no closure during a fatigue cycle. On the Closure Load versus Cycles graphs (Figures 17, 19, 24, and 27), when closure load is plotted on the minimum load line, closure is at or below the minimum load.

Since there was no closure when the specimen reached threshold crack growth rate, ΔK_{th} equals ΔK_{effth} (2.44). This value of ΔK_{effth} agrees within 1.0% of the ΔK_{effth} values from the reference study's constant R tests (3:10).

The crack growth rate (see Figure 18) for the constant K_{max} increasing K_{min} portion of this test behaved as expected. The initial crack growth rate is very close to the growth rate curve for the the reference study's $R = 0.1$ decreasing ΔK crack growth rate curve shown on the figure. As the stress ratio increased, the crack growth curve gradually moved toward
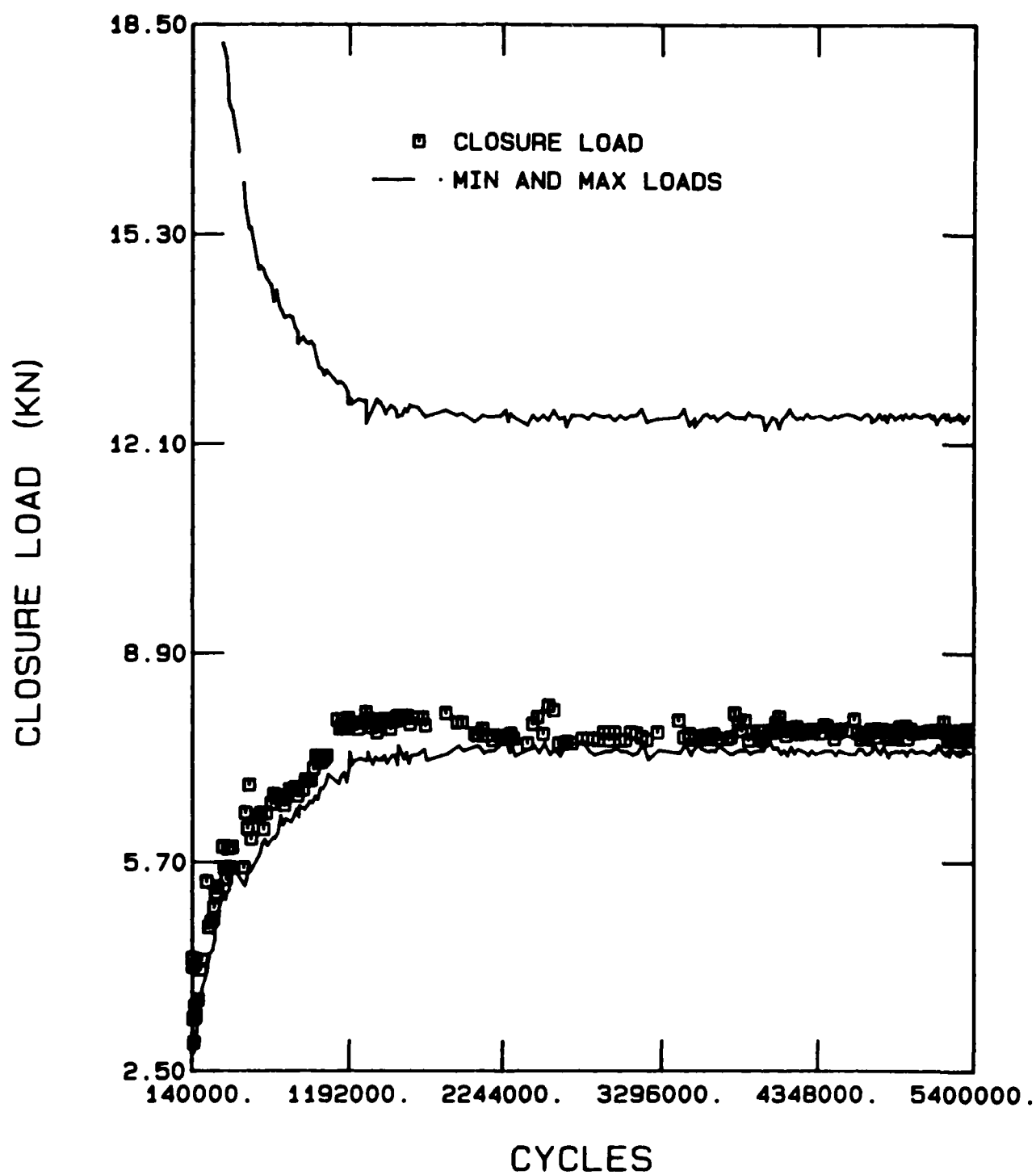
40

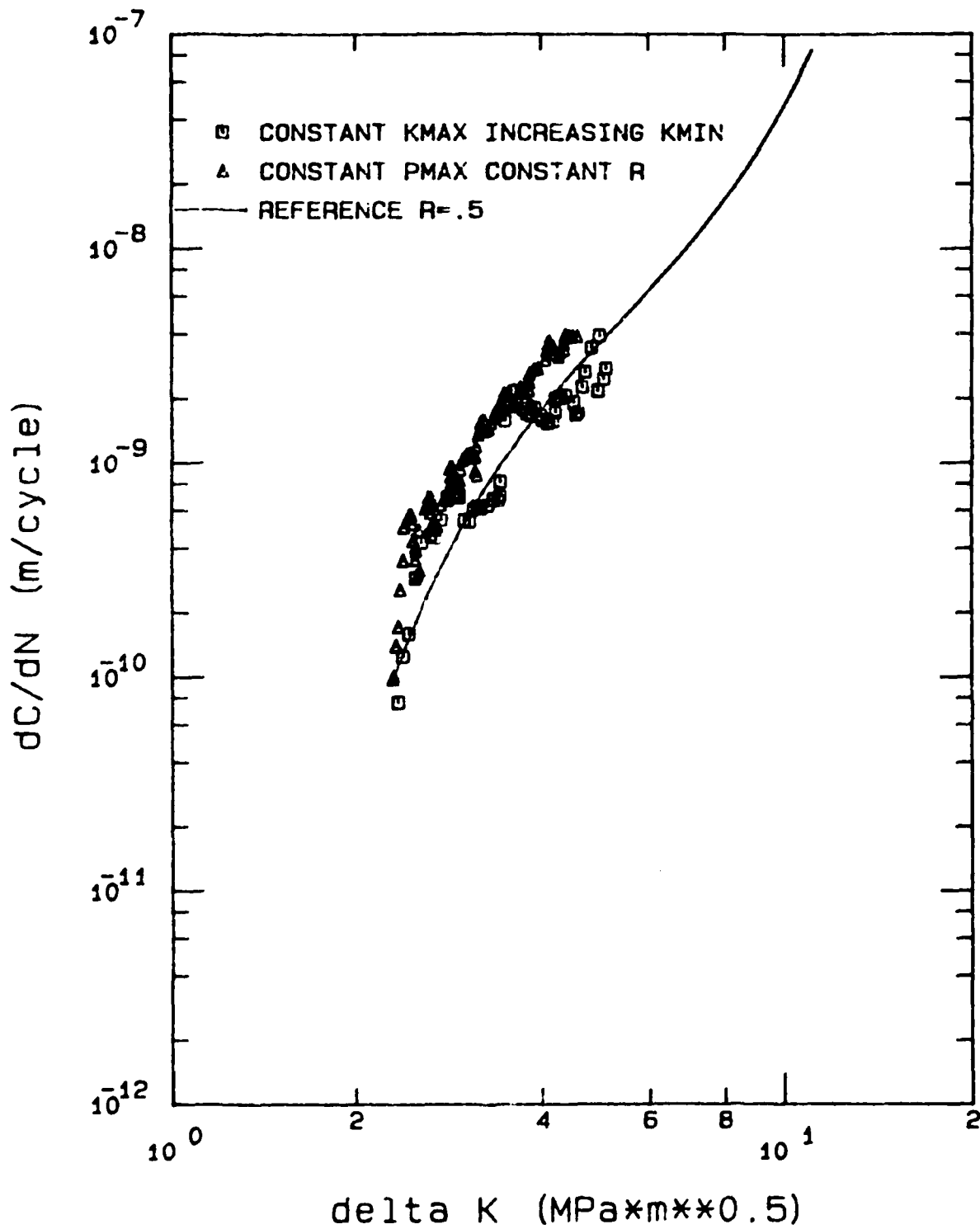Figure 17.   Specimen 86002 Closure Load vs. Cycles

41

Figure 18. Specimen 86002 ΔK vs. Crack Growth Rate

42

the reference study's R = 0.5 crack growth curve and finally crossed it as the crack growth rate reached the threshold level at R = 0.6.

Initially, there was significant scatter in the closure data between the stress ratios of 0.2 and 0.4. The individual load displacement curves in this region had to be re-examined to see if the calculated closure loads actually existed or if there was a problem with the closure measurement method. There appeared to be no closure in this region and Figure 17 was adjusted to indicate this.

Specimen 86003 was also precracked at R = -1.0. The constant K_{max} increasing K_{min} test (Figure 11) for this specimen started with a stress ratio of R = -0.3. The threshold crack growth rate was reached at R = 0.44.

With the initial stress ratio at -0.3, closure was expected to develop during the start of the test. Figure 19 shows that there was significant closure during the start of the test. As the stress ratio increased, the closure load fell below minimum load. There was more scatter on this plot of Closure Load versus Cycles between R = 0.2 and 0.4. The load displacement curves for this section of the test did not indicate closure was present. Figure 19 was adjusted to reflect this.

Figure 20 shows the crack growth rate for this test plotted versus ∆K. The initial part of this curve does not show the true growth rate. The data reduction program for this test does not allow for negative stress ratios. The initial
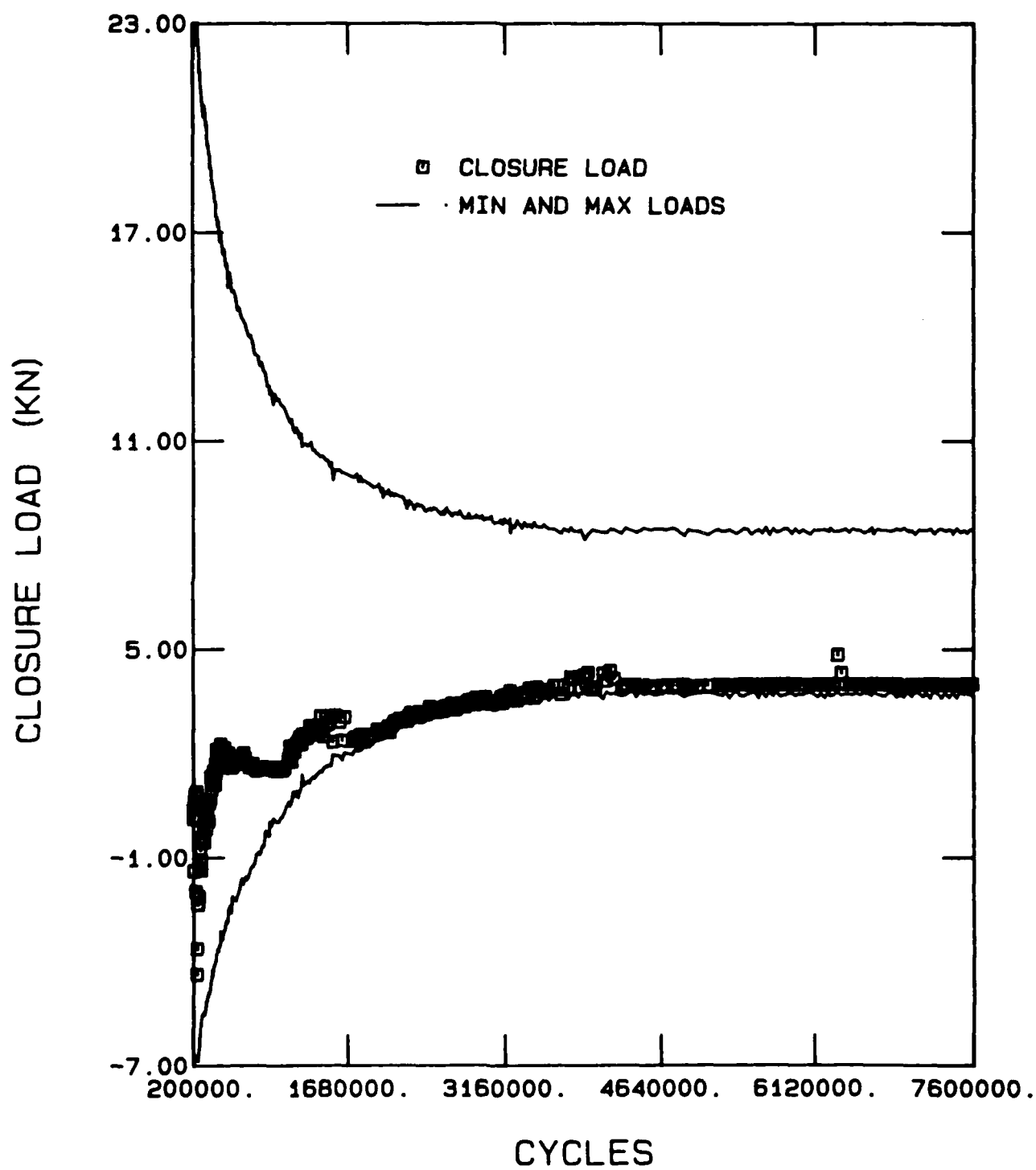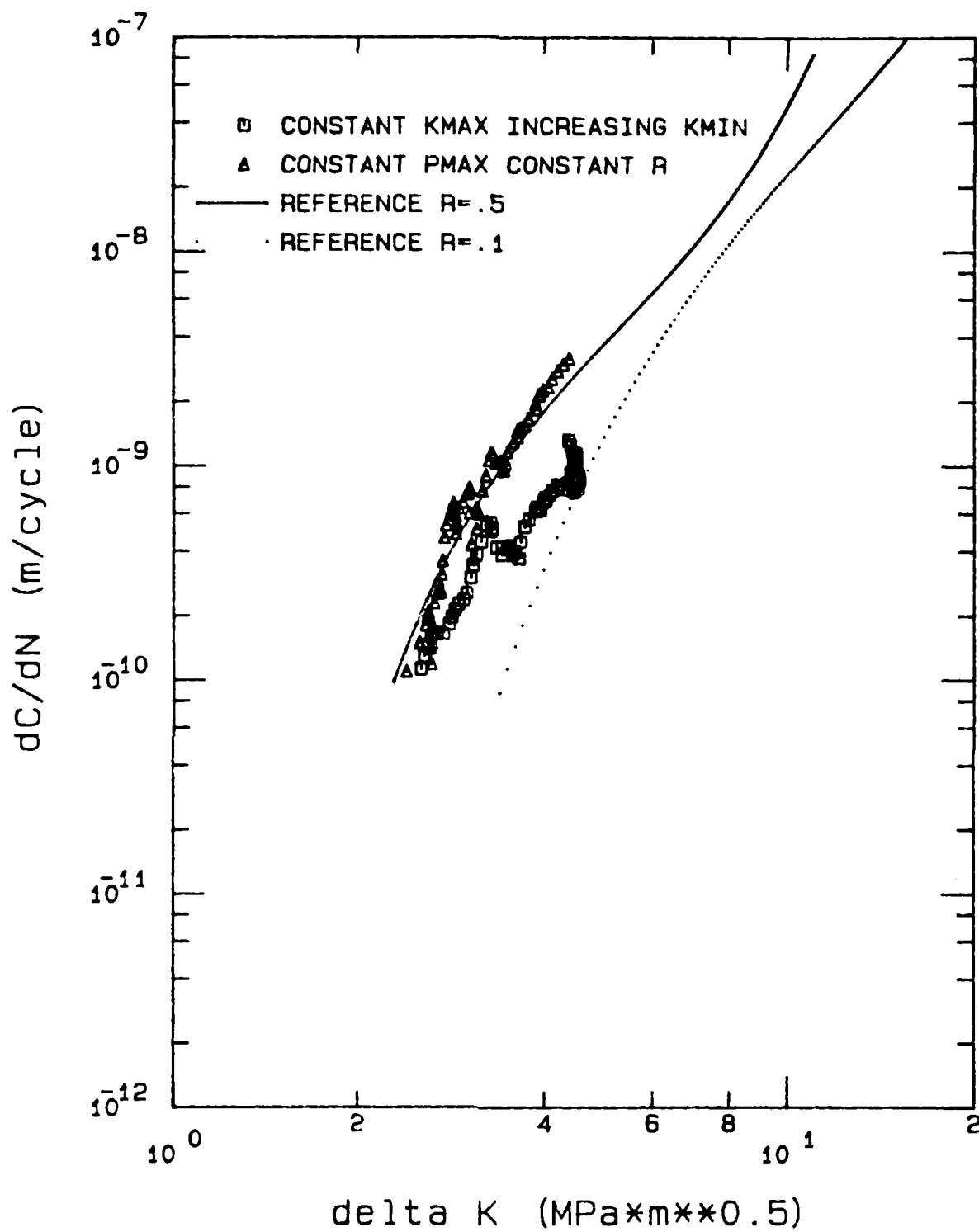
43

Figure 19.   Specimen 86003 Closure Load vs. Cycles

44

Figure 20.   Specimen 86003 ΔK vs. Crack Growth Rate

45

stress ratios for this test were reset to zero by the IBM 9000 which resulted in the vertical line crack growth curve at the beginning of the test.

Figure 21 shows the same crack growth rate curves adjusted for closure and plotted versus ΔK_{effth}. The crack growth curves for both the constant K_{max} increasing K_{min} test and constant P_{max} constant R test shifted to the left and agreed with the reference study's R = 0.5 crack growth curve in the $1*10^{-10}$ to $1*10^{-9}$ m/cycle crack growth rate region. This is similar to what occured for the reference study's constant R tests. The value of ΔK_{effth} for this test was 2.54. This value agrees with the reference study's ΔK_{effth} values within 3.6% (3:10).

Figure 22 plots the applied and effective threshold intensities for the constant K_{max} increasing K_{min} tests conducted in this study along with the decreasing ΔK tests conducted in the reference study (3:10). The trend indicates a dependence of ΔK_{th} on stress ratio but a ΔK_{effth} which is independent on stress ratio.
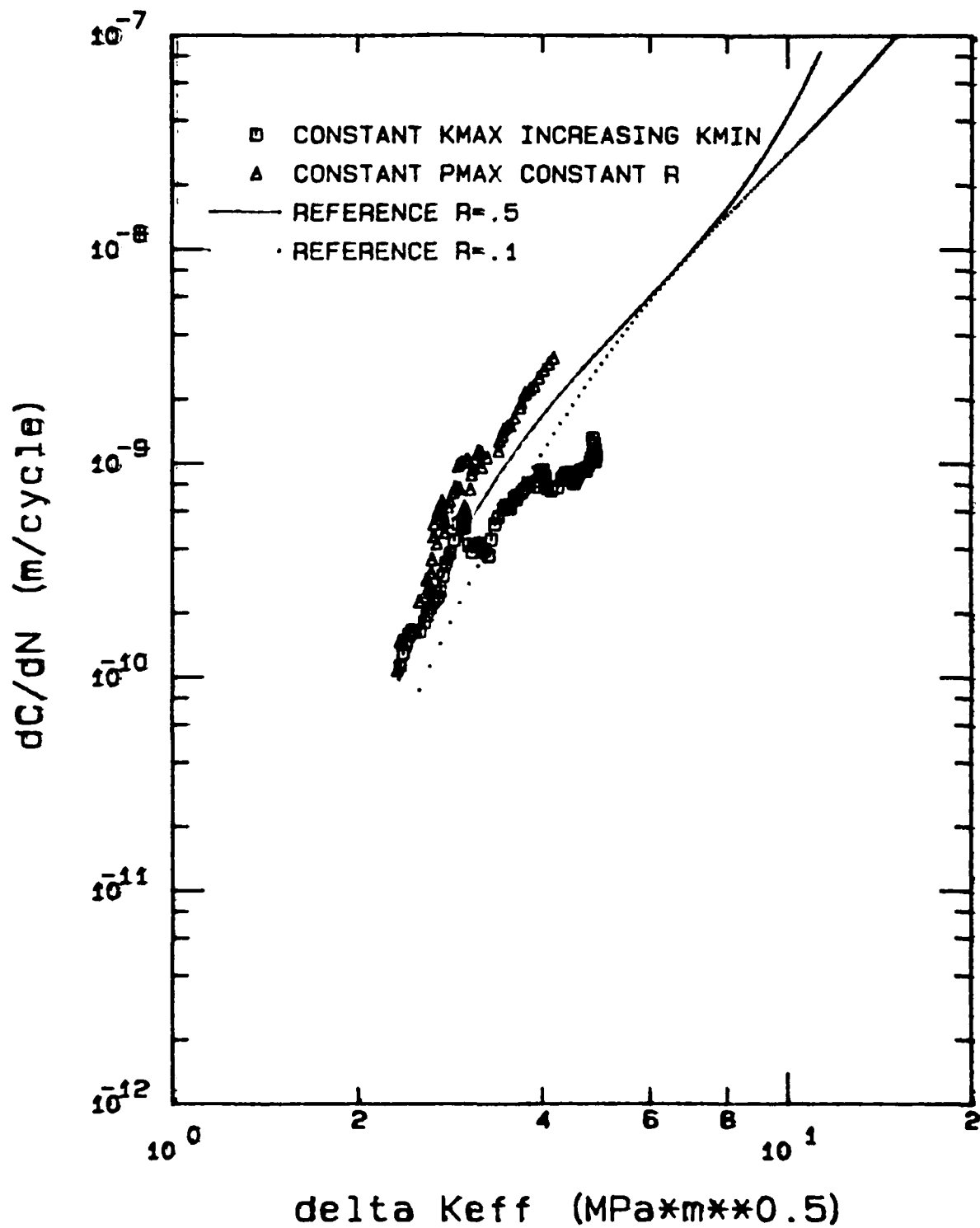
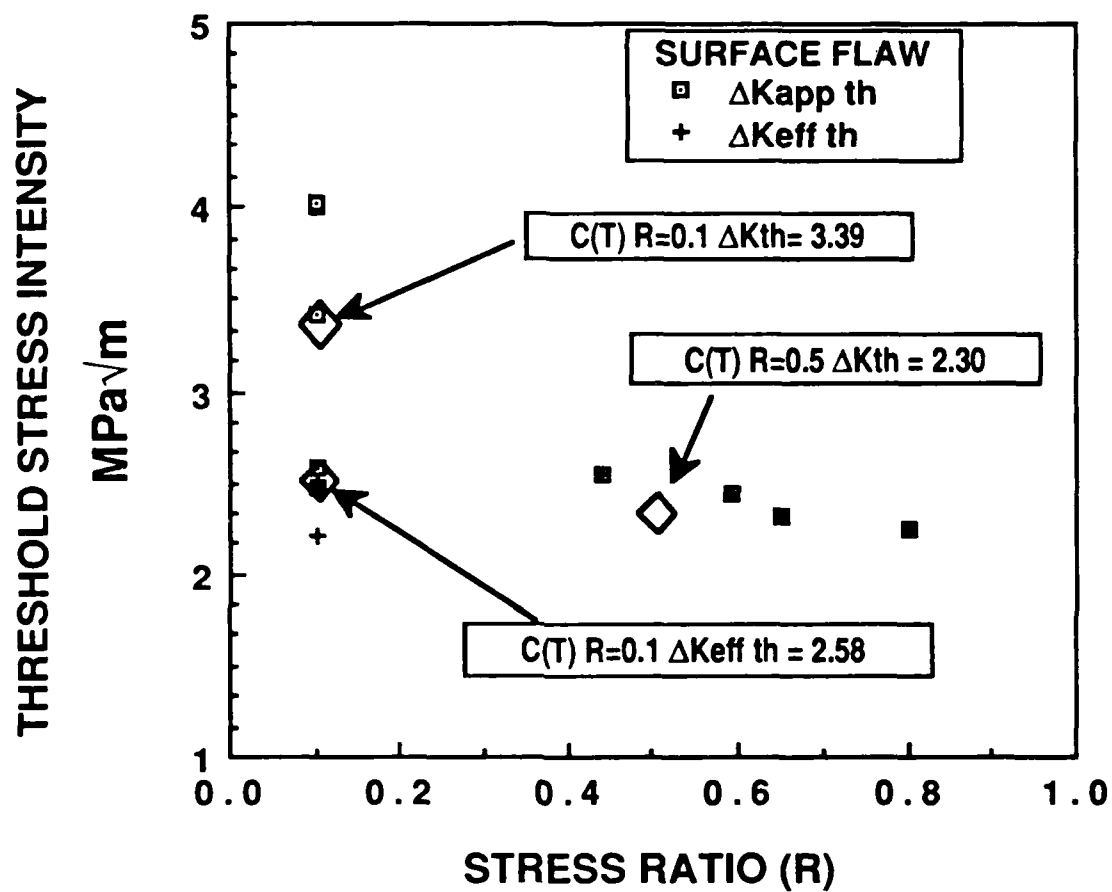Figure 21. Specimen 86003 ΔK_{eff} vs. Crack Growth Rate

Figure 22. ΔK_{th} and ΔK_{effth} vs. Stress Ratio for Decreasing ΔK Tests (Constant R Decreasing ΔK Tests Values from 3:10)

48

Constant K_{max} Decreasing K_{min} Tests

For these tests, a block of 198,000 cycles was applied to the specimen for each stress ratio. Thirty data points were taken during the block of cycles and a straight line was fit to the thirty points to calculate the crack growth rate. If the crack growth rate was below the threshold level, the stress ratio was decreased and another block of cycles was applied (Figure 12). This process was continued until the threshold crack growth rate level of $5*10^{-11}$ m/cycle was reached. 198,000 cycles were applied during each block of cycles to allow the crack to grow a sufficient amount that the IDG would be able to measure any crack growth that may occur within its 2 μm resolution capability.

The laser IDG is capable of accurately measuring crack growth rates below the threshold growth rate level of $1*10^{-10}$ m/cycle used for the tests which had initially growing cracks with slowly decreasing crack growth rates approaching the threshold growth rate level (decreasing ΔK test and constant K_{max} increasing K_{min} test). To save time and get a more precise determination of when the crack actually started to grow, the threshold crack growth rate level was changed to $5*10^{-11}$ m/cycle for the constant K_{max} decreasing K_{min} tests.

Specimen 86010 was precracked at R = -1.0. The first block of cycles applied to the specimen was at a stress ratio of R = .70. Crack growth rate first went above the threshold level at a stress ratio of R = 0.64 (see Figure 23). The ΔK_{th} value for this specimen was 2.22.
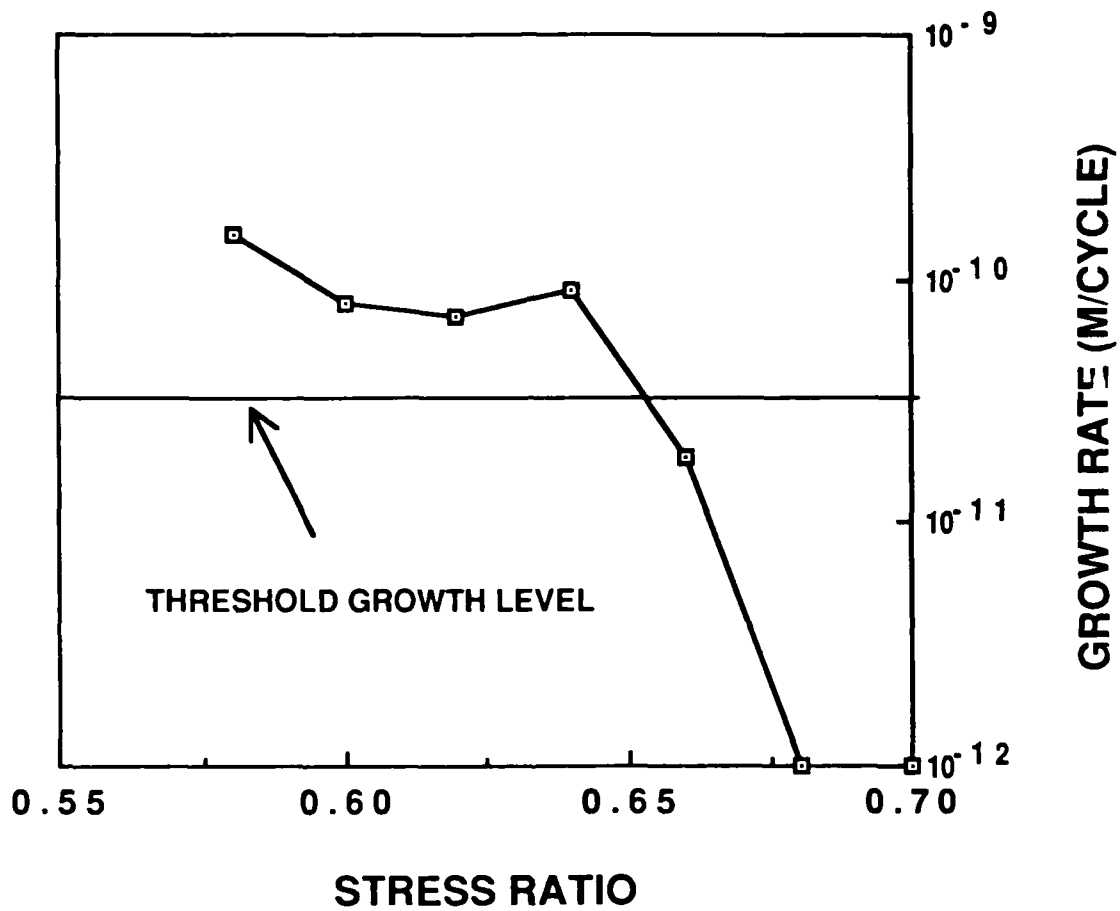
49

Figure 23. Specimen 86010 Growth Rate vs. Stress Ratio

There were three more blocks of cycles applied to the specimen after reaching threshold crack growth rate. The IBM 9000 computed crack growth for the block of cycles by fitting a polynomial to the thirty data points taken during the block of cycles. This was the only available data during the test and this method did not measure threshold growth until a stress ratio of R = 0.58. The crack growth rates for Figure 23 were computed by fitting a straight line to the thirty data points. The straight line fit appears to be a better indicator of the actual crack growth rate for the block of cycles.

The stress ratios for this test were large and closure was not expected to develop. Figure 24 shows that there was no measureable closure during the entire test. Since there was no closure ΔK_{th} equals ΔK_{effth} (2.22). This value agrees within 9.3% of the reference study's ΔK_{effth} values (3:10).

Figure 25 shows the crack growth rate curve for the specimen during the constant P_{max} constant R portion of the test along with the measured crack growth rates for each block of cycles. The constant P_{max} constant R crack growth rate curve behaved as expected, staying just to the left of the reference study's R = 0.5 crack growth rate curve.

Specimen 86020 was precracked at a stress ratio of R = -1.0. The initial stress ratio for the constant K_{max} decreasing K_{min} test was R = 0.44. Threshold crack growth rate occured at a stress ratio of R = .21 (see Figure 26).

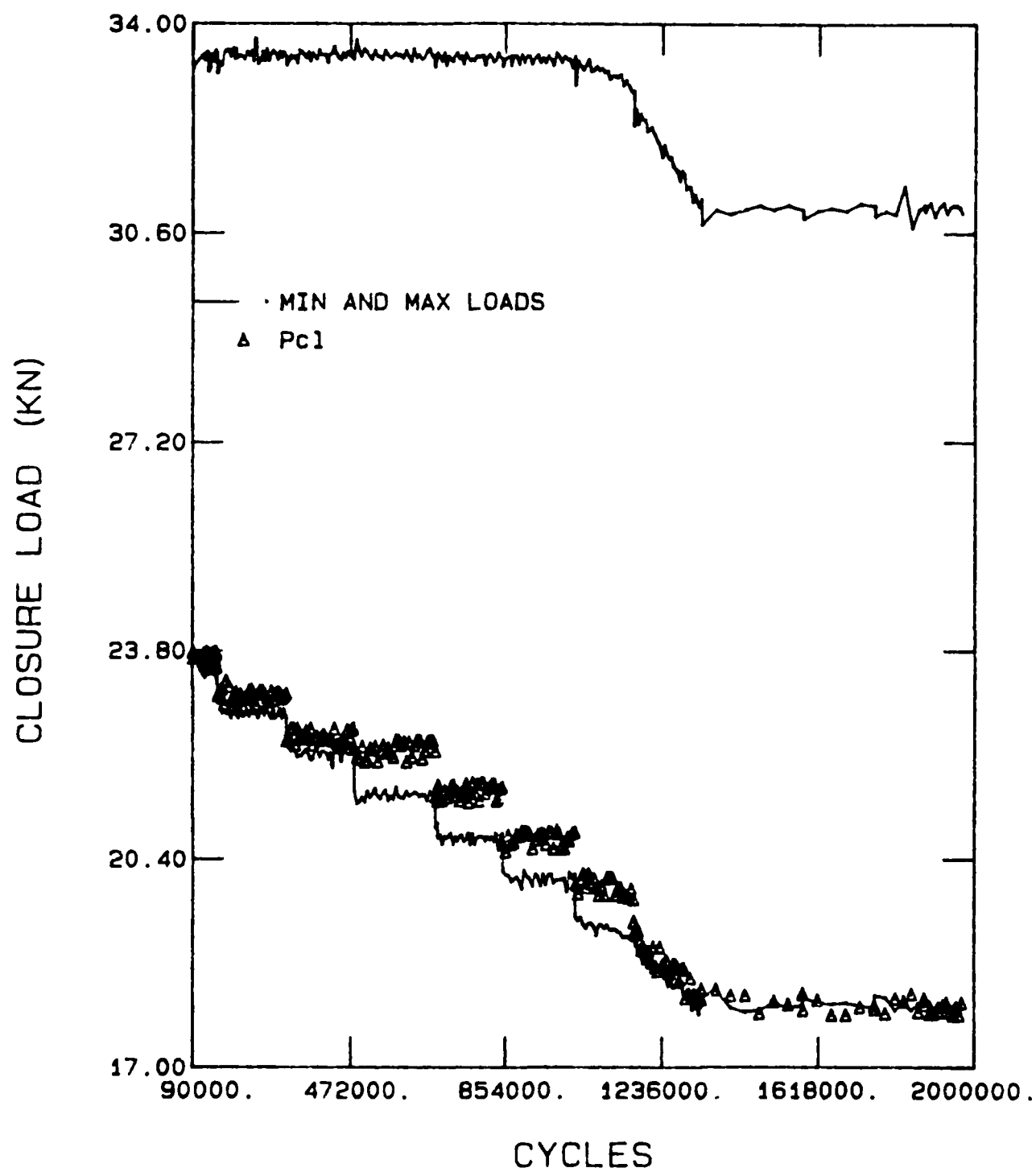Since the initial stress ratios were large, closure was not expected to develop, but as the stress ratios decreased to

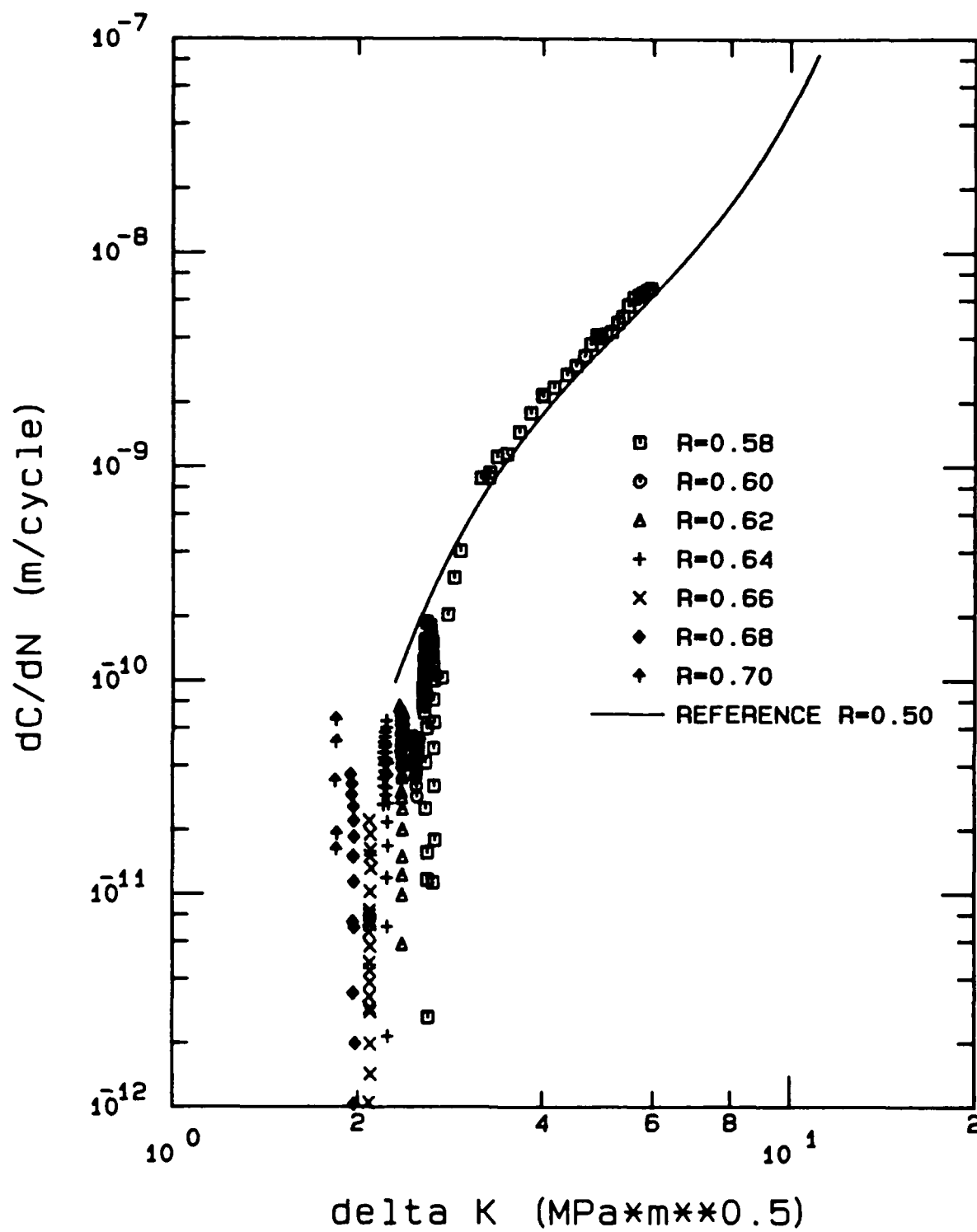Figure 24.   Specimen 86010 Closure Load vs. Cycles

52

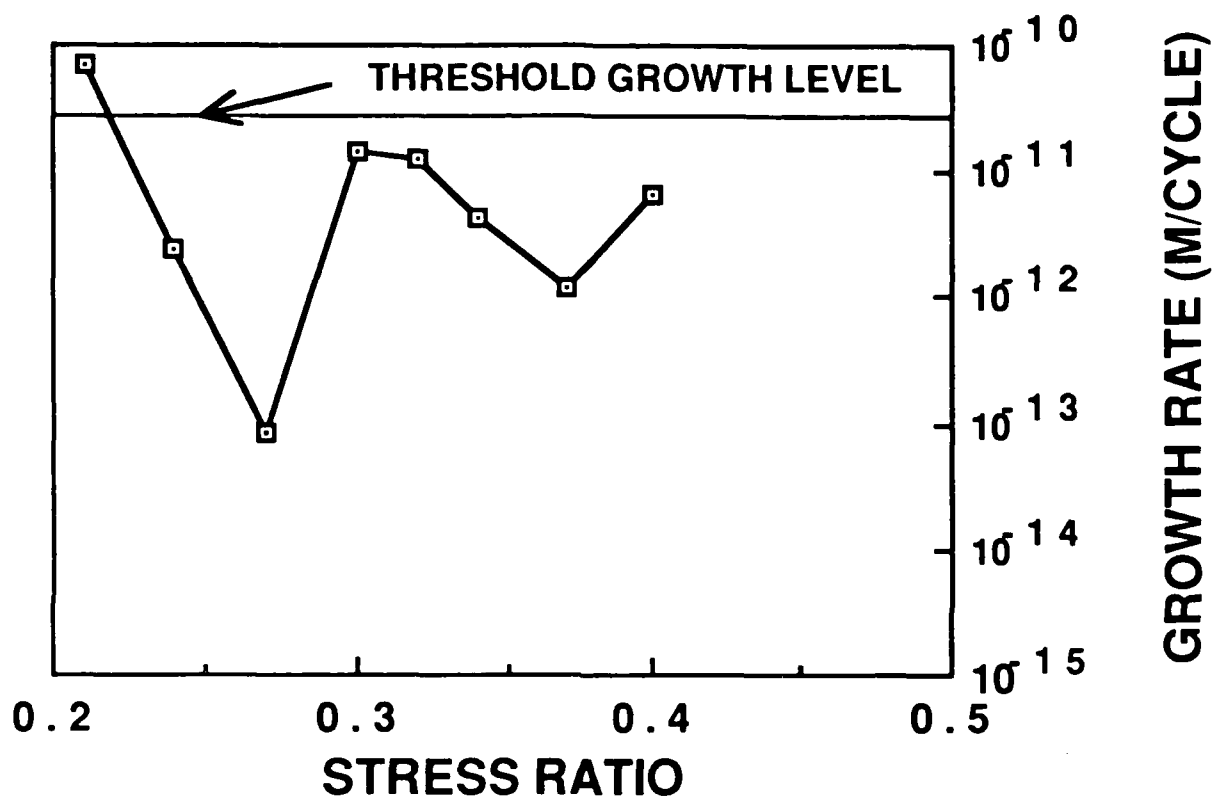Figure 25. Specimen 86010 ΔK vs. Crack Growth Rate

Figure 26. Specimen 86020 Growth Rate vs. Stress Ratio

54

R = 0.21 closure should develop in the specimen. Figure 27 shows that there was was no measured closure for the entire test. This resulted in a ΔK_{effth} value well above all other measured values (3.03) for this study and the reference study. It is important to note that there was considerable scatter of the closure load values in the same area as other tests, between the stress ratios of R= 0.2 and 0.4. In examining these points, there did not seem to be any closure, however based on the previous tests it appears that the laser IDG had trouble measuring closure at the crack tip of a surface flaw specimen in the region between obvious no closure development (R ≥ 0.5) and areas of definite closure (R ≤ 0.1). If there was closure present during the test and the laser IDG could not detect it, this would explain the ΔK_{effth} value for this test being well above the previous ΔK_{effth} values. If there was closure present at the crack tips, then the resulting ΔK_{effth} would be smaller and closer to the expected values.

Figure 28 shows the crack growth rate plotted versus ΔK. The crack growth rates for each block of cycles are shown as well as the crack growth rate curve for the constant maximum load constant stress ratio (0.21) portion of the test. The crack growth rate curve behaved as expected, staying between the reference test curves with stress ratios of 0.5 and 0.1.

Figure 29 shows the threshold stress intensities plotted versus the stress ratios for the two constant K_{max} increasing K_{min} tests from this study and for the constant R tests conducted previously in the reference tests. This graph shows

55
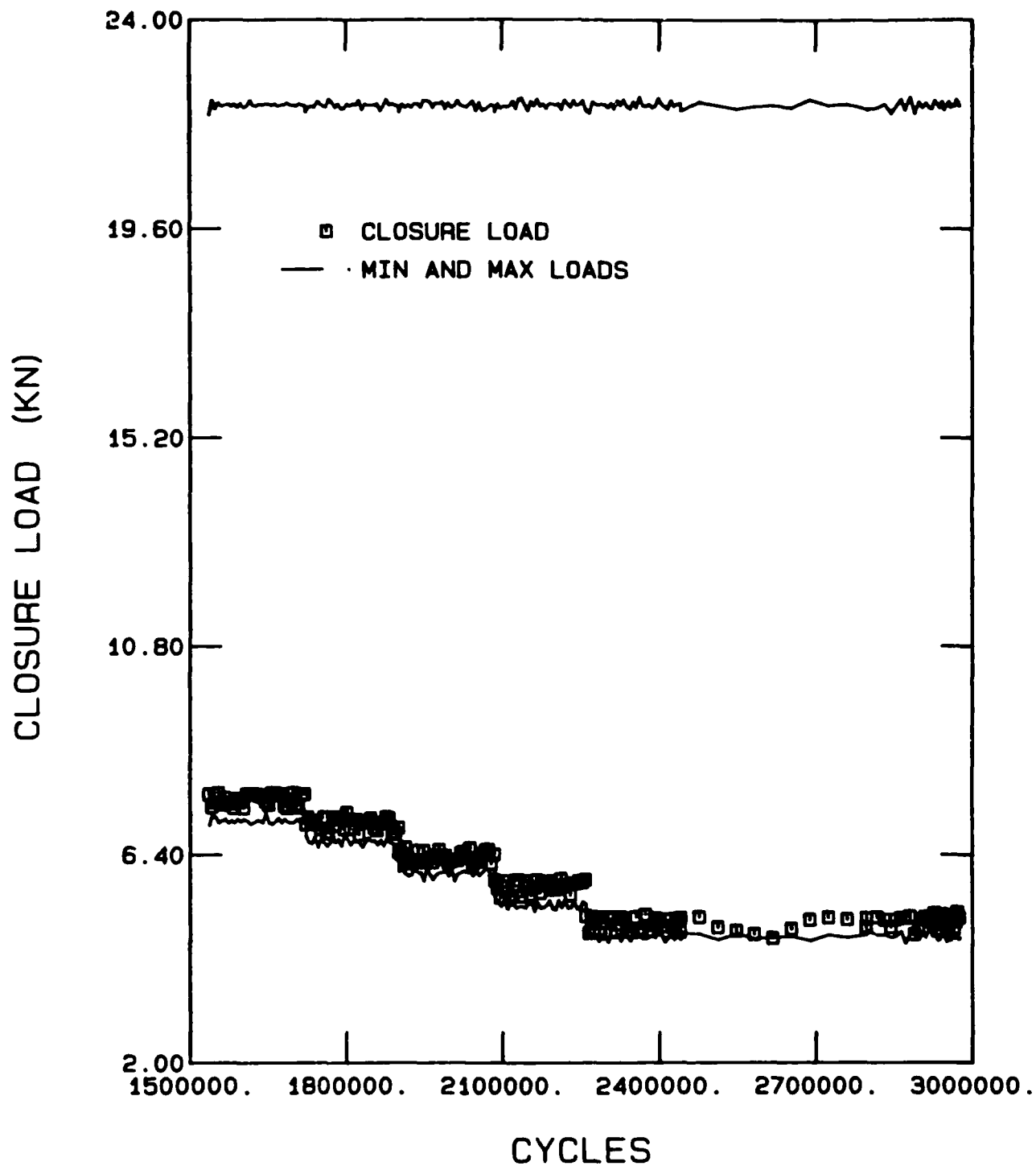
Figure 27. Specimen 86020 Closure Load vs. Cycles

56
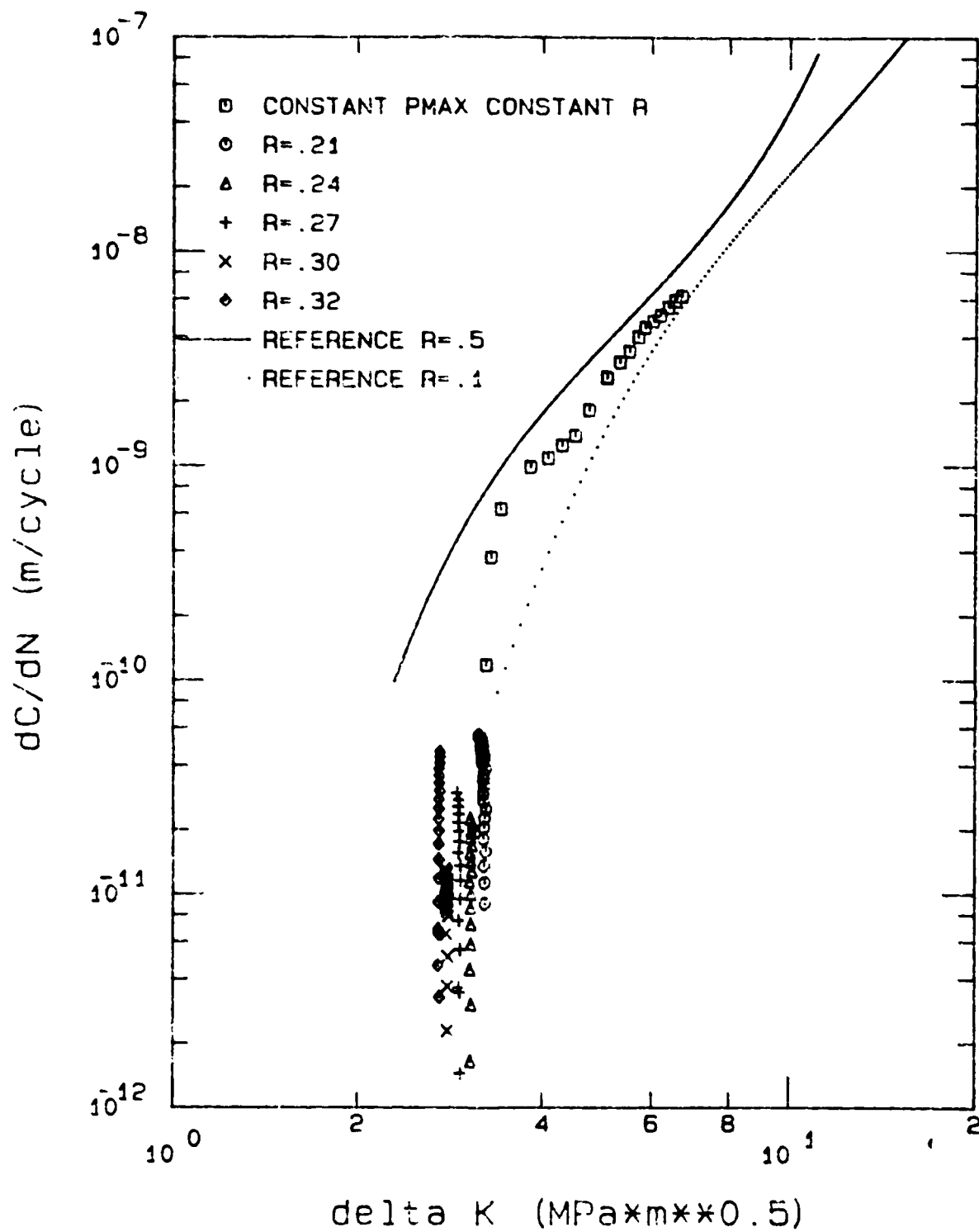
Figure 28. Specimen 86020 ΔK vs. Crack Growth Rate

57
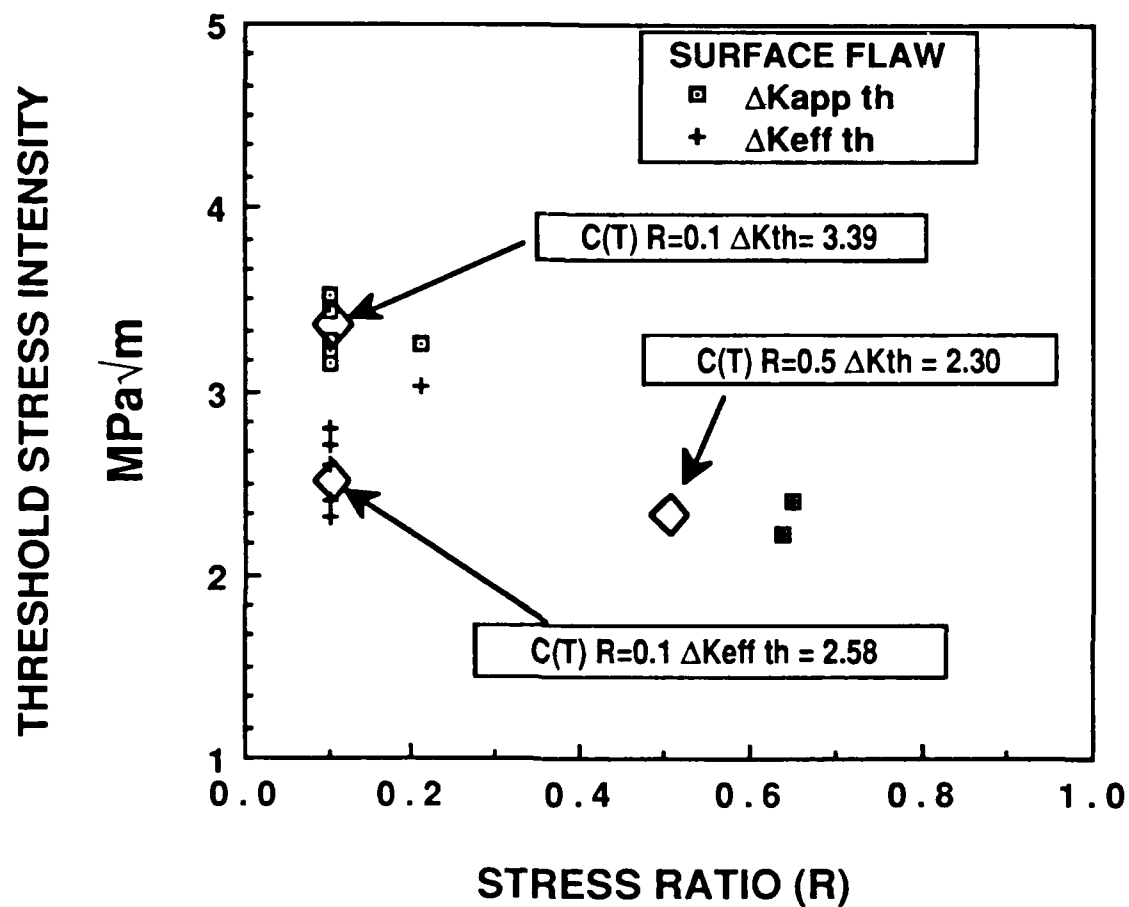
Figure 29. ΔK_{th} and ΔK_{effth} vs. Stress Ratio for Increasing ΔK Tests (Constant R Increasing ΔK Values from 3:10)

58

the same trend that developed for the decreasing ΔK tests. ΔK_{appth} varies with stress ratio while ΔK_{effth} is relatively constant. Figure 30 is a compilation of all four threshold test types discussed in this paper. Figure 30 shows the same trends as discussed above.

Figure 30. ΔK_{th} and ΔK_{effth} vs. Stress Ratio for All Tests
(Constant R Test Values from 3:10)

V. Conclusions

This study was conducted to examine the effects of loading history, closure loads, and changing stress ratios on crack growth in the near-threshold region for a Ti-Al alloy. Previous tests had examined threshold crack growth for this material using constant stress ratio.

These previous reference tests concluded that crack growth curves for this material, with different stress ratios, merged to one material crack growth curve when plotted versus ΔK_{eff}. These tests also concluded that the material seemed to have a constant value for ΔK_{effth} (3:6).

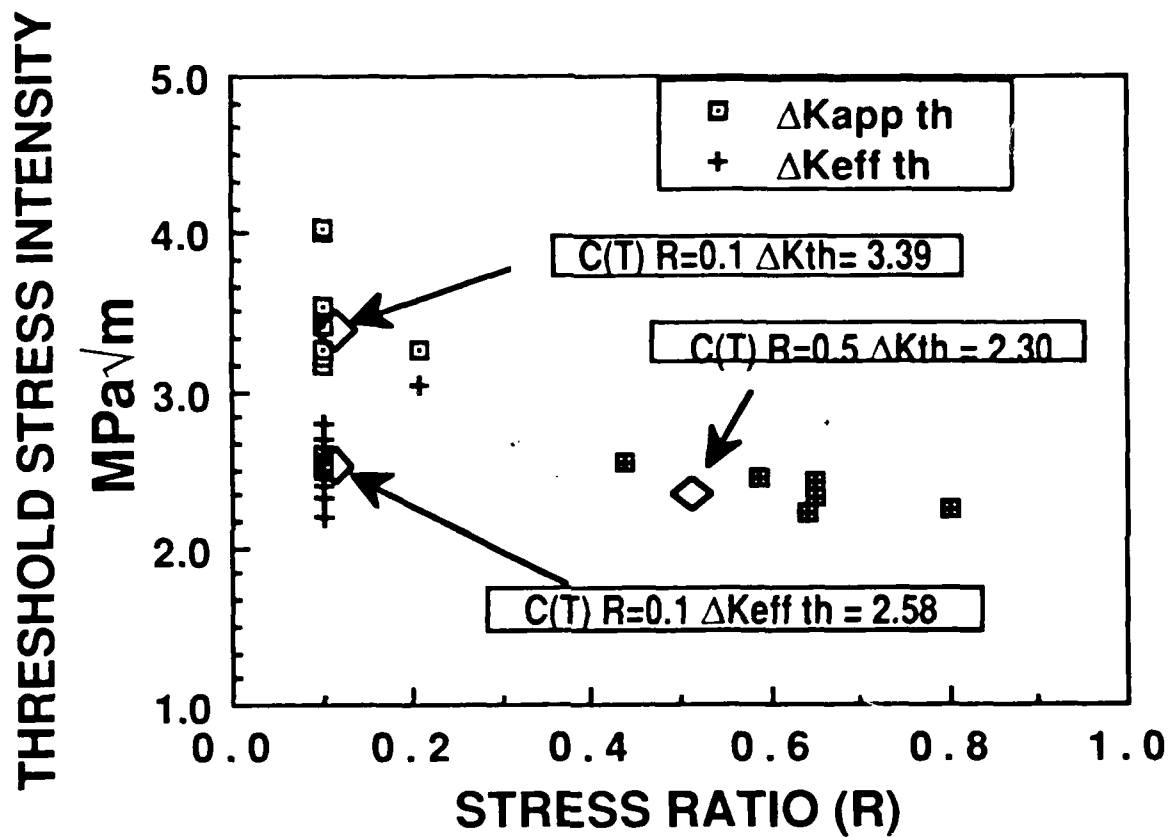To examine the effects of different loading histories, closure loads, and stress ratios, two types of constant K_{max} tests were conducted. The first constant K_{max} test increased K_{min}, and hence R, with crack growth until the threshold crack growth rate was reached (Figure 2a). The second constant K_{max} test decreased K_{min}, and therefore R, with each block of applied cycles until the crack growth rate reached the threshold level (Figure 2b).

A summary of the conclusions for this study are:

1. When the crack growth rate curves are adjusted for closure and plotted versus ΔK_{eff}, they coincide only in the near-threshold region ($1*10^{-9}$ m/cycle to $1*10^{-10}$ m/cycle).

2. ΔK_{th} is dependent on stress ratio.

3. ΔK_{effth} values are not dependent on loading history and are approximately equal for different stress ratios.

61

4. The laser interferometer displacement gage was not able to accurately measure crack closure loads at the tips of the surface flaw in certain regions. For small stress ratios ($R \leq 0.1$) and large closure loads, or large stress ratios ($R \geq 0.5$) and no closure, the IDG accurately measured closure. At stress ratios between 0.1 and 0.5, the IDG did not accurately detect closure.

5. Plastic zone size appears to have very little effect on near-threshold crack growth rate. The constant R decreasing K_{min} tests produced plastic zones which decreased with crack growth. The constant K_{max} increasing K_{min} tests maintained a constant plastic zone size as the crack grew. The constant R and constant load tests produced increasing plastic zone sizes with crack growth . All three test types had identical near-threshold growth rates when there was no closure or when plotted versus ΔK_{eff}.

Bibliography

1. Ritchie, R. O. "Thresholds For Fatigue Crack Propagation: Questions and Anomalies," *Advances in Fracture Research* (Fracture 84): 248 (1984).

2. Cadman, A. J., Brook, R., and Nicholson, C. E. "Effect of Test Technique on the Fatigue Threshold ΔK_{th}," *Concept and Measurement*: 59-75 (1981).

3. Jira, J. R., Weerasooriya, T., Nicholas, T., and Larsen, J. M. "Effects of Closure on the Fatigue Crack Growth of Small Surface Cracks in a High-Strength Titanium Alloy," submitted for *Fatigue 87* by AFWAL/MLLN, Wright-Patterson AFB, Ohio, 1987.

4. Paris, P. C., and Erdogan, F. "A Critical Analysis of Crack Propagation Laws," *Journal of Basic Engineering*, Transaction ASME: 528-534 (1963).

5. Elber, W. "Fatigue Crack Closure Under Cycle Tension," *Engineering Fracture Mechanics*, Vol. 2: 40 (1970).

6. Ritchie, R. O., Suresh, S., and Moss, C. M. "Near-Threshold Fatigue Crack Growth in 2 1/4Cr-1Mo Pressure Vessel Steel in Air and Hydrogen," *Journal of Engineering Materials and Technology*, Transactions of the ASME, Vol. 102: 293-299 (1980).

7. Walker, N. and Beevers, C. J. "A Fatigue Crack Closure Mechanism in Titanium," *Fatigue of Engineering Materials and Structures*, Vol. 1: 135-148 (1979).

8. Elber, W. "Significance of Fatigue Crack Closure, Damage Tolerance in Aircraft Structures," *ASTM STP 486*: 230-242 (1971).

9. Banerjee, S. A Review of Crack Closure, Interim Report for Period August 1983 Through December 1983.

10. Davenport, R. T., and Brock, R. "The Threshold Stress Intensity Range in Fatigue," Fatigue Material Structures, Vol. I: (1979).

11. Allison, J. E., "The Influence of Slip Character and Microstructure on Fatigue Crack Growth in Alpha and Alpha & Beta Titanium Alloys", Ph.D. Thesis, Carnegie-Mellon University, 1982.

12. Fleck, N.A., Smith, I. F. C., and Smith, R. A. "Closure Behavior of Surface Cracks," Fatigue of Engineering Materials and Structures: 225-239, (1983).

13. Jolles, M. "Constraint Effects on the Prediction of Fatigue Life Surface Flaws," Journal of Engineering Materials and Technology, Vol. 105: 215-218 (1983).

14. Carter, D., W., Canda, W. R., and Blind, J. A. "Surface Flaw Crack Growth in Plates of Finite Thickness", USAFA/DFEM, 1987.

15. Prodan, M., Erismann, T. H., "Fatigue Growth of Part-Through Cracks: A New Approach," Advances in Fracture Research Vol. 3: 1924-1934 (1984).

16. Raju, I. S., and Newman, J. C. "Stress Intensity Factors for an Elliptical Surface Flaw," Engineering Fracture Mechanics Vol. 11: 817 (1979).

17. Irwin, G. R. "The Crack Extension Force for a Part-Through Crack in a Plate," Journal of Applied Mechanics: 651-654 (1962).

18. Döker, H., Bachmann, V., and Marci, G. "A Comparison of Different Methods of Determination of the Threshold for Fatigue Crack Propagation," Concept and Measurement: 45-57 (1981).

19. Herman, W. A., Hertzberg, R. W., Newton, C. H., and Jaccard, R., "A Re-evaluation of Fatigue Threshold Test Methods", Fatigue 87, Vol. II: 819-828 (1987).

20. Sharpe, W. N. , Jr., "Interferometric Surface Strain Measurement", International Journal of Nondestructive Testing: 1-10 (1971).

21. Hartman, G., and Nicholas, T. "An Enhanced Laser Interferometer for Precise Displacement Measurements," Experimental Techniques, Vol. 11: 24-26 (1987).

22. Mattheck, C., Moravietz, P., and Munz, D. "Stress Intensity Factor at the Deepest Point of a Semi-Elliptical Surface Crack in Plates Under Stress Gradients," International Journal of Fracture, Vol. 23: 201-212 (1983).

VITA

Captain Dale A. Nagy was born on 30 August 1956 in Pittsburgh, Pennsylvania. He graduated from high school in Pittsburgh, Pennsylvania, in 1974 and attended the U.S. Air Force Academy, from which he received the degree of Bachelor of Science in Aeronautical Engineering in May 1978. He completed pilot training and received his wings in August 1979. He then served as an F-4 Wild Weasel pilot and instructor pilot in the 81st Tactical Fighter Squadron, Spangdahlem AB, Germany. In 1984 he served as an instructor pilot and flight examiner for the 562nd Tactical Fighter Training Squadron, George AFB, California until entering the School of Engineering, Air Force Institute of Technology, in May 1986.

        Permanent address: 10306 N.W. 6th Street

                                Plantation, Florida 33324

REPORT DOCUMENTATION PAGE		Form Approved OMB No. 0704-0188

1a REPORT SECURITY CLASSIFICATION UNCLASSIFIED	1b RESTRICTIVE MARKINGS None

2a. SECURITY CLASSIFICATION AUTHORITY	3. DISTRIBUTION/AVAILABILITY OF REPORT
2b. DECLASSIFICATION/DOWNGRADING SCHEDULE	Approved for public release; Distribution unlimited

4 PERFORMING ORGANIZATION REPORT NUMBER(S) AFIT/GAE/AA/87D-13	5 MONITORING ORGANIZATION REPORT NUMBER(S)

6a NAME OF PERFORMING ORGANIZATION School of Engineering	6b OFFICE SYMBOL (If applicable) AFIT/ENY	7a NAME OF MONITORING ORGANIZATION

6c. ADDRESS (City, State, and ZIP Code) Air Force Institute of Technology Wright-Patterson AFB OH 45433-6583	7b ADDRESS (City, State, and ZIP Code)

8a. NAME OF FUNDING/SPONSORING ORGANIZATION Air Force Wright Aero Lab	8b OFFICE SYMBOL (If applicable) MLLN	9 PROCUREMENT INSTRUMENT IDENTIFICATION NUMBER

8c. ADDRESS (City, State, and ZIP Code) AFWAL/MLLN Wright-Patterson AFB OH 45433-6583	10 SOURCE OF FUNDING NUMBERS			
	PROGRAM ELEMENT NO	PROJECT NO	TASK NO	WORK UNIT ACCESSION NO

11 TITLE (Include Security Classification)

See Box 19

12. PERSONAL AUTHOR(S)
Dale A. Nagy, Capt, USAF

13a TYPE OF REPORT MS Thesis	13b TIME COVERED FROM _____ TO _____	14. DATE OF REPORT (Year, Month, Day) 1987 December	15 PAGE COUNT 74

16. SUPPLEMENTARY NOTATION

17 COSATI CODES			18 SUBJECT TERMS (Continue on reverse if necessary and identify by block number)
FIELD	GROUP	SUB-GROUP	Threshold Crack Growth Rate, Stress Intensity Factor
20	11		Closure Load

19 ABSTRACT (Continue on reverse if necessary and identify by block number)

TITLE: THRESHOLD FATIGUE CRACK GROWTH IN Ti-6Al-2Sn-4Zr-6Mo

Thesis Chairman: Dr S Mall
Professor of Aeronautics and Astronautics

20 DISTRIBUTION/AVAILABILITY OF ABSTRACT ☒ UNCLASSIFIED/UNLIMITED ☐ SAME AS RPT ☐ DTIC USERS	21 ABSTRACT SECURITY CLASSIFICATION UNCLASSIFIED
22a NAME OF RESPONSIBLE INDIVIDUAL Dr S Mall, Professor	22b TELEPHONE (Include Area Code) 513-255-2998	22c OFFICE SYMBOL AFIT/ENY

DD Form 1473, JUN 86   Previous editions are obsolete   SECURITY CLASSIFICATION OF THIS PAGE

19. The purpose of this study was to examine the effects of different loading histories, closure loads, and stress ratios on the near-threshold crack growth rate of a Ti-Al alloy. Two different types were conducted on four separate specimens to determine the threshold stress intensity factor of thr material. The first test type maintained a constant maximum stress intensity factor, K_{max}, on a specimen with a growing crack. As the specimen grew, the minimum stress intensity factor was increased until the crack growth rate reached the threshold level ($1*10^{-10}$ m/cycle). The second test type also maintained a constant K_{max}. For this test a block of cycles was applied to the specimen and if the crack growth rate for the block of cycles was below the threshold level then K_{min} was decreased by a small amount and another block of cycles was applied. This process was continued until the crack growth rate reached the threshold level. Once the threshold stress intensity factor was determined the cracks were grown under constant maximum load and constant stress ratio (R) to measure the threshold crack growth rate. Both test types were conducted over a wide range of stress ratios to investigate the effects of varying closure loads.

An MTS machine was used to apply the fatigue cycles to the specimen and a laser interferometer displacement gage (IDG) was used to measure compliance crack growth rate and the closure loads for the specimen.

The results of these tests indicate that threshold stress intensity factors were dependent on the stress ratio. Threshold stress intensity factors adjusted for closure (effective threshold stress intensity factors) were not dependent on stress ratio.

The crack growth rate curves for all tests coincided in the near-threshold region ($1*10^{-9}$ to $1*10^{-10}$ m/cycle) when plotted versus effective threshold stress intensity factor. Finally, the laser IDG had difficulty measuring closure loads while transitioning from a condition of large closure loads (low stress ratio) to a condition of no closure (high stress ratio).

END

DATE
3 - 88

DTIC